Exploring the Wireless Sensor Node Tradespace within Structural Health Monitoring

by

George Clernon

B. Eng. Electronics, University of Limerick, 1997

SUBMITTED TO THE SYSTEM DESIGN AND MANAGEMENT PROGRAM IN PARTIAL FULFILLMENT OF THE REQUIREMENTS FOR THE DEGREE OF

MASTER OF SCIENCE IN ENGINEERING AND MANAGEMENT

AT THE

MASSACHUSETTS INSTITUTE OF TECHNOLOGY
JUNE 2015

Signature of Author________________________ Signature redacted

George Clernon
System Design and Management Program
May 8th 2015

Certified and Accepted by________________ Signature redacted

Patrick Hale
Executive Director, System Design and Management Program
Massachusetts Institute of Technology

This page intentionally left blank

Exploring the Wireless Sensor Node Tradespace within Structural Health Monitoring

by

George Clernon

Submitted to the System Design and Management Program on May 8th, 2015 in Partial Fulfillment of the Requirements for the Degree of Master of Science in Engineering and Management

Abstract

Historically, Structural Health Monitoring (SHM) involved visually or acoustically observing a structure and if damage was detected, remedial action was undertaken to repair or replace it. For example, as early as 6,500 BC, potters were known to listen for audible sounds during the cooling of their ceramics, signifying structural failure. In 1864 the UK parliament legislated for dam monitoring after a dam failure lead to the deaths of 254 people. The Golden Gate and Bay Bridges in San Francisco were monitored by Dean S. Carder in 1937 to determine "the probabilities of damage due to resonance" during an earthquake. Given the technological limitations of the last century, the predominant focus of SHM has been on identifying and understanding the global modal properties of a structure. However, the promise of SHM is the detection of any damage to infrastructure at the earliest possible moment from an array of sensors and actuators. To achieve this goal, not only global but local facets of the structure must be monitored. If this promise is realized, it will be possible to design bridges closer to their tolerances, to extend their operational lives, and to switch servicing to more cost-effective condition based maintenance. Such changes will reduce construction and maintenance costs while still providing the same level of service. This thesis will explore the wireless sensor node tradespace with the specific intent of delving into the areas limiting large scale, high density, localized coverage of structural health monitoring of bridges.

Thesis Supervisor: Patrick Hale
Title: Executive Director, System Design and Management Program

This page intentionally left blank

Acknowledgements

I would like to thank Gerd Melder for encouraging me to consider the MIT System Design and Management Program back in 2013 when I was looking for a program that combined engineering and management. I am very grateful to you for securing management approval to sponsor my time at MIT.

Once this journey began I met many inspiring students in both the SDM '14 and '15 cohorts. Special thanks goes to Hann, my partner on nearly all team based projects and homework assignments since IAP, and to Somwang, Tobias and Dave with whom I spent countless hours over the past 18 months.

My thanks to Pat Hale and the SDM staff for producing a wonderful program that lays bare the most challenging aspects of engineering and management to its students.

My eternal gratitude goes to my family, especially to my parents, Eddie and Alice, for your unwavering support.

To my wife, Cherry, thank you for your love, support, and patience. Without you, I would never have completed this program. And to Eoin, thank you for filling my free time with Duplo blocks, Thomas the Tank Engine and heartfelt fun.

And to my late brother, Eddie, you were a life-long learner and have inspired me to be the same. On the evening of commencement, the day before your birthday, we will toast your memory with a drop or two of Midleton Very Rare Irish Whiskey. A most fitting way to close this amazing journey.

This page intentionally left blank

Table of Contents

List of Figures

List of Tables

This page intentionally left blank

Introduction

At its core, Structural Health Monitoring (SHM) is a continuous system identification of a physical or parametric model of a structure using time-dependent data [1]. SHM has been used to monitor aerospace, civil, and mechanical infrastructure including bridges, pipelines, railways, buildings, helicopters, and airplanes. The signals gathered from the monitored structure include vibrations (movement, displacement), acoustic emissions (cracking), impedance (cracking, corrosion), distance (displacement), and strain (stress, strain). As all damage begins at the material level [2], it is critical to establish a baseline system model against which models built on future data will be compared.

Historically, SHM involved visually or acoustically observing the structure and if damage was detected, remedial action to repair or replace was undertaken. For example, as early as 6,500 BC, potters were known to listen for audible sounds during the cooling of their ceramics, signifying structural failure [3]. One of the first legislated requirements for structural health monitoring was put in place by the parliament of the UK in 1864 after a 30m dam failed. 254 lives were lost as a result of the failure. The legislation has been updated over time and as late as 1975 gives "a supervising engineer the responsibility for continual surveillance of a reservoir and dam, including the keeping and interpretation of operational data" [1]. Bridges also have a long history of being monitored. The Golden Gate and Bay Bridges in San Francisco were monitored by Dean S. Carder in 1937 with "the principal object ... to determine, if possible, the probabilities of damage due to resonance ... at the time of an earthquake" [4]. Another example is offshore oil installations where the cost of manual inspection by divers and the regulatory requirements for inspection, beginning in the 1970s, lead to innovations in the area of "dynamic characteristics and load-response mechanisms" [1]. In the 1990s, helicopter manufacturers began to implement SHM on "the engine, transmission, gears, bearings and drive shafts" using vibration monitoring techniques [5]. And in the 2000s, many academic researchers developed wireless sensor networks on bridges and other civil infrastructure thereby greatly reducing the cost of SHM for large structures [6], [7]. As noted in Figure 1, research interest in SHM has grown over time but may have peaked in 2010. However, SHM for bridges has steadily increased in the same period.

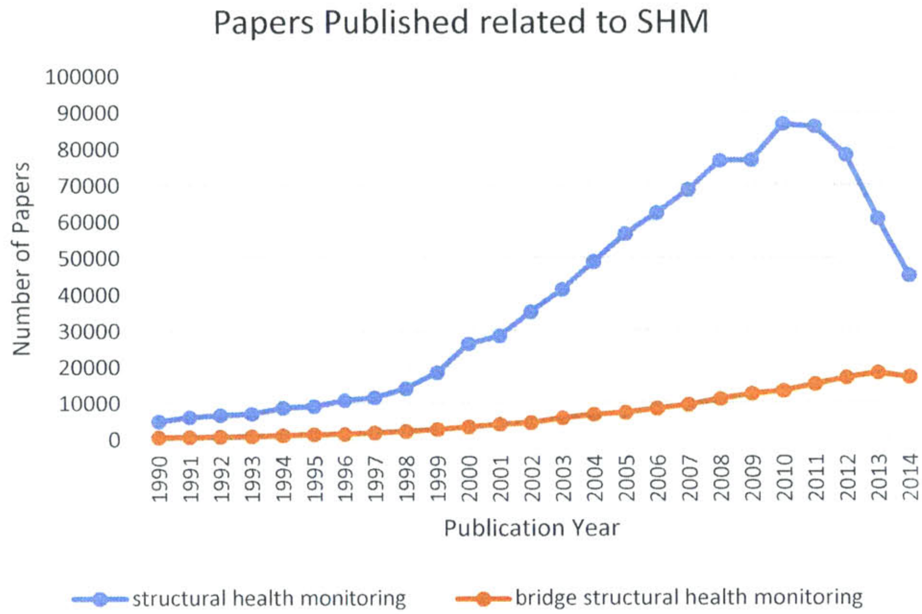

Figure 1: Number of Papers Published per Year with "Structural Health Monitoring" in the paper[1]

While SHM has a long history, it is part of a wider set of disciplines of "which monitoring and assessing damage are principal concerns" [8]:

- Structural Health Monitoring
- Condition Monitoring
- Non-Destructive Evaluation
- Statistical Process Control

Condition Monitoring (CM) is very similar to SHM but focuses on rotating and reciprocating machinery. Non-Destructive Evaluation (NDE) is normally carried out offline and after the damage has been detected by online sensors. NDE is used to characterize the severity of damage. Statistical Process Control monitors the output of the sensors and raises "out of band" events if sensor data exceed preset trigger values. As SHM develops sensing and actuating capabilities along with increased computational processing power at the sensing node, it is beginning to incorporate features of CM, NDE, and SPC.

---

[1] The numbers were calculated from searching Google Scholar (24/Apr/2015) for occurrences of "Structural Health Monitoring" and "Bridges Structural Health Monitoring" between 1990 and 2014.

The promise of SHM is the detection of damage to infrastructure at the earliest possible moment. To achieve this goal, not only global but local facets of the structure must be monitored. If this promise is realized, it will be possible to design bridges closer to their tolerances, to extend the operational life of machinery, and to switch equipment servicing to more cost-effective condition based maintenance. Such changes will reduce construction, machinery, and maintenance costs while still providing the same level of service.

Structural Health Monitoring of Bridges

The field for SHM is very broad so in order to narrow it, the sub-topic of SHM of Bridges was selected. Bridges provide several areas worth considering; it is an area of growing interest for academics (Figure 1), it has constraints that discount the use of certain types of monitoring solutions, and it is regularly in the news due to the current state of infrastructure in the US. Although some new bridges in the US are being designed to have an operational lifetime of 100 years and are constructed with SHM sensors embedded into the structure (c.f. I-35W Bridge crossing the Mississippi River in Minneapolis, Minnesota), over 20% of bridges in the US have been classified as deficient by the Federal Highway Administration [9].

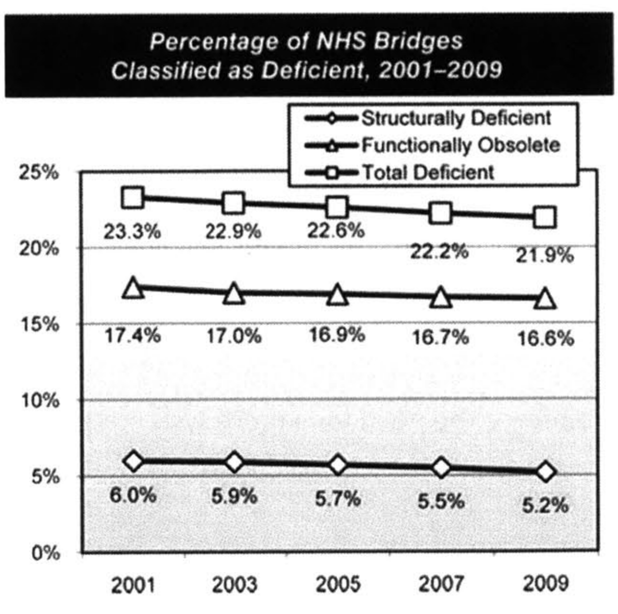

Figure 2: Percentage of National Highway System Bridges Classified as Deficient, 2001-2009 [9]

Although, the number of deficient bridges is slowly decreasing, it still amounts to 132,124 bridges out of 603,310. There "was a backlog of potentially cost-beneficial bridge investments in 2008 of

$121.2 billion" [9]. In order to eliminate the deficient backlog by 2028, the US would have to increase annual spending on the backlog from $12.8bn to $20.5bn [10]. The American Society of Civil Engineers assigned bridge infrastructure a C+ grade in its 2013 Report Card for America's Infrastructure [10]. Over 500 failures of bridge structures between 1989 and 2000 were studied by Wardhana and Hadipriono [11] with 9.5% of failures caused by Deterioration or Fatigue. With nearly 50 bridge failures in a decade, it only takes one failure like that of the I-35W Saint Anthony Falls Bridge collapse in 2007 to raise awareness of the limitations in current SHM procedures. This bridge collapse killed 13 people and injured 145. The bridge had been classified as structurally deficient in 2005 and it was scheduled to be replaced in 2020. Unfortunately, the true state of the structure was revealed during rush-hour traffic on August 1st, 2007 when it collapsed at 6.05pm.

Every two years every bridge in the highway system is visually inspected as part of the National Bridge Inspection Program (NBIP). This program was created in 1971 after a bridge failed resulting in the deaths of 46 people. Unfortunately, the nature of visual inspection means it is not very effective. Visual inspection relies on the expertize of the inspector and on the defects to be visible on the surface of the structure. For example, despite regular maintenance, it was only during intrusive inspections in 2009 that the deteriorated state of roller bearings in the bridge piers of the Hammersmith Flyover in London was discovered [12]. It is not only bridges that require visual inspection, it is mandated that after major earthquakes structures must undergo detailed visual inspection before they can be reoccupied. This means buildings can remain closed for days after the event. It has been estimated the cost of inspecting "the connections of steel moment frame buildings was between $200 and $1000 per welded connection" after the Northridge earthquake of 1994 [6]. These events reinforce the need for a more systematic way for evaluating the health of civil infrastructure.

With all of the attention given to structurally deficient bridges in the past couple of decades it should not be surprising to see academic interest in Bridge SHM grow overtime. Similar to the more general SHM, Bridge SHM may have hit a peak but a little later in 2013 (Figure 3)[2].

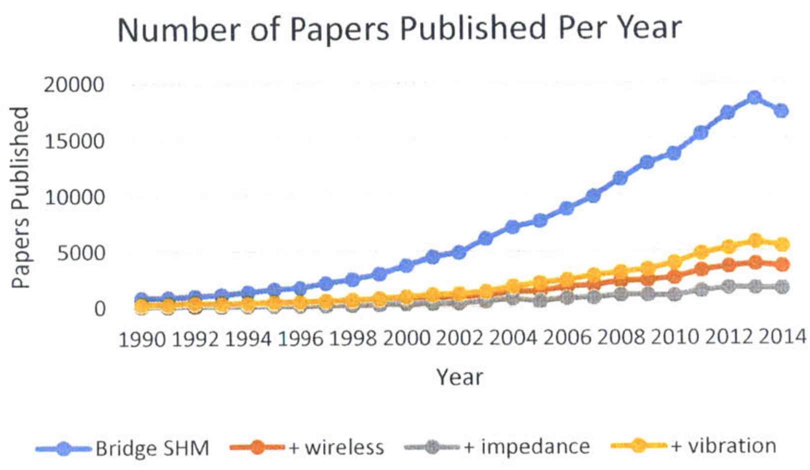

Figure 3: Number of Papers Published Per Year with Bridge SHM

It is also worth noting that overtime commercial applications of bridge SHM have moved from demonstration to greater numbers of design confirmation and lifetime extension. This trend (Figure 4) was found in a study of 40 SHM installations across the globe [13].

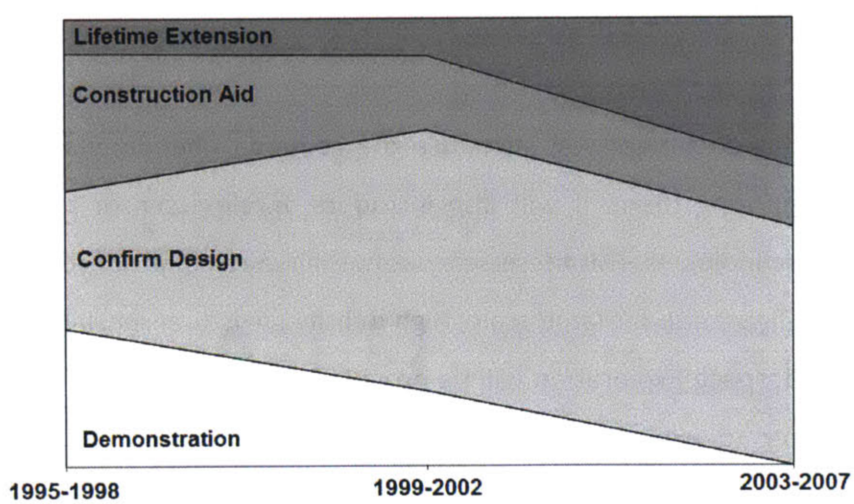

Figure 4: Time Evolution of the Reasons for Monitoring [13]

[2] The numbers were calculated from searching Google Scholar (24/Apr/2015) for occurrences of "Bridge Structural Health Monitoring" between 1990 and 2014. The '+' elements were appended individually to the main Bridge SHM search term.

These projects were carried out over a 22 year period with most projects costing under $50k but if the installation was to be permanent and autonomous the cost increased to between $100k and $500k. Projects with 10 or fewer sensors dominated the list while those with greater than 50 sensors amounted to only 8.

The greatest impediment to wider adoption of SHM for bridges is cost. The new I-35W bridge was instrumented with 323 wired sensors embedded into the structure. The cost of this installation was $1m (0.5% of the bridge construction budget). Although the wired sensor cost of $3100 has decreased over time, it is still significant. Of the 1,400 to 4,000 new bridges added per year in the US [11], not many of them are $234m projects like that of the I-35W reconstruction project. For new or refurbished structures a $1m price tag for 323 sensors may be excessive. Given the Federal Highway administration estimate of a $121bn deficient backlog of bridge work, it averages $1m per project. If 1% of the project cost was allocated to instrumenting the bridge this would give a budget of $10,000 thus a per sensor cost of $100-$200 for 50-100 sensors depending on the size of the project. At this cost range and volume of sensors, only wireless sensor nodes are practical. With a bill of materials cost at $100 (c.f. costs listed in the *Components and their Parameters* section below) the goal of blanketing a bridge in sensors measuring localized events may have a little further to go before it is viable in the market place.

Document Structure

The remainder of this document will introduce the common phenomena monitored and the techniques for monitoring them. It will also introduce wireless sensor networks (WSN) and energy harvesting technologies. This thesis sets out to examine a couple of concepts to determine the best system configuration for large scale, high density structural sensing. An introduction to Multi-Attribute Tradespace Exploration will be provided along with details how it was modified and applied in order to explore the wireless sensor node tradespace of structural health monitoring. As part of those details the various components making up a sensor network will be examined and a model of the tradespace will be constructed. An examination of the results of the tradespace exploration will highlight where the concepts have addressed current limitations of WSNs. The document will close with a summary and suggestions for future work in this area.

Structural Health Monitoring of Bridges

According to Modares & Waksmanski [14], SHM systems are used to

1. Record structural behavior
2. Identify defects for the prevention of failure events
3. Provide information for the planning of inspection and maintenance activities
4. Verify design during construction process
5. Ensure long-term quality of structure

By providing an up to date model of the structures health, maintenance can shift from a scheduled based activity to a condition based activity; that is, infrastructure owners can respond "just in time" to address issues thus potentially reducing maintenance and inspection costs as well as conduct remedial activities in a timely manner. In order to achieve this always-on type of monitoring one must determine local failures along with the current practice of identifying global facets. Lynch [6] attributed the predominant interest in global modal properties to the cost of deploying sensor nodes. Unfortunately, global modal properties are susceptible to environmental factors which reduce their effectiveness for damage assessment. If lower cost sensor nodes were available it would be possible to increase sensor densities thereby increasing monitoring fidelity which in turn will provide insight into local structural health and will lead to localized damage identification. Autonomous wireless sensor nodes have the potential to sense many of the local modal properties, process the data locally, and send information to a central location while in operation for 10 or more years.

Monitored Phenomena

In order to construct both global and local models of a structure significant amounts of data is required. The data includes but is not limited to the following information: geographic information of the bridge site; location, type, and performance of sensors; recording date and time; and results of damage identification [14]. This data is gathered for every sensor node regardless of phenomenon being sensed. Table 1 provides a list of phenomena and a sample of measurement mechanisms.

Parameter	Sensor	Type	Accuracy (%)	Sensing Range	Operating temperature (°C)
Corrosion	Acoustic emission	Noncontact	±0.1	0.07–40 cm	−65 to 176
	Corrosion sensors	Contact	±0.05	up to 8.9 cm	−40 to 60
	Fiber optics	Contact	±0.02	up to 50 cm	−40 to 79
Cracking	Acoustic emission	Noncontact	±0.1	0.07–40 cm	−100.6 to 176
	Crack meter	Contact	±0.25 to ±1	1.3–30 cm	−20 to 80
	Thermography	Noncontact	±2	0.02–0.07 cm	−40 to 2,000
Displacement	Fiber optics	Contact	±0.02	up to 30 cm	−40 to 79
	Global positioning system	Noncontact	±1.3 to ±3.6	from 0.5 cm	−55 to 65
	Joint meters	Contact	±0.25 to ±1	1.3–30 cm	−20 to 80
	Laser scanning	Noncontact	±3	up to 1 m	0 to 40
	LVDTs	Contact	±0.1 to ±0.3	±101 cm	−55 to 70
	Linear potentiometers	Contact	±1	±121 cm	−65 to 105
	Photographic devices	Noncontact	±0.2	from 3 cm	−20 to 70
Fatigue	Fatigue sensor	Contact	Unspecified	Unspecified	Unspecified
Force	Load cell	Contact	±0.05 to ±1	44.5–889,600 N	−28 to 93
Settlement	Settlement gauge	Contact	±0.1 to ±0.5	0.5–70 m	−20 to 80
	Settlement cell	Contact	±0.1	1.5–64 m	−20 to 80
Strain	Fiber optics	Contact	±0.02	±10,000 $\mu\varepsilon$	−40 to 79
	Foil strain gauge	Contact	±0.1 to ±1	±40,000 $\mu\varepsilon$	−270 to 370
	Semiconductor strain gauge	Contact	±0.25 to ±1.5	±3,000 $\mu\varepsilon$	−50 to 150
	Vibrating wire strain gauge	Contact	±0.1 to ±0.5	±3,000 $\mu\varepsilon$	−28 to 104
Temperature	Fiber optics	Contact	±0.2 to ±0.5	−40 to 79°C	−40 to 79
	Thermocouples	Contact	±1 to ±2	−200 to 2,600°C	−200 to 2,600
	Thermography	Noncontact	±2	−40 to 2,000°C	−40 to 2,000
	Thermoresistors	Contact	±0.15 to ±0.3	−200 to 650°C	−200 to 650
Tilt	Capacitive tilt meter	Contact	±0.5 to ±2	±0.5° to ±50°	−40 to 85
Vibration	Capacitive accelerometer	Contact	±1	±20,000*g*	−40 to 185
	Piezoelectric accelerometer	Contact	±0.02 to ±1	±80,000*g*	−40 to 135
	Laser Doppler vibrometer	Noncontact	±0.05 to ±1	±10,000*g*	0 to 40
Water level	Piezometer	Contact	±0.1 to ±0.25	0–149 MPa	−20 to 80
Wind	Anemoscope	Contact	±2 to ±3	0–270 km/h	−550 to 700

Table 1: Sensors Used in Bridge Monitoring Organized by Parameter Type [14]

Of these phenomena, a smaller subset will be examined and included in the tradespace exploration. The selected phenomena are Corrosion, Crack, Displacement, Strain, Vibration, Temperature and Humidity. Each phenomenon and proposed measurement mechanisms are discussed below.

Cracking

The most common mechanism for measuring cracking is acoustic emissions. Acoustic emission measurement can be undertaken passively or actively. Passive acoustic emission measurements utilize a piezoelectric transducer to listen for the energy emitted by changes in the material under test. This energy is emitted in the form of high frequency waves. When the piezoelectric transducer is perturbed it will generate an output voltage waveform which can be recorded and analyzed (Figure 5). Active acoustic emission measurement works in a similar way but requires two transducers, one to emit an ultrasonic wave and the other to receive it. With piezoelectric transducers it is possible to use one transducer to both send and receive the wave but this configuration does not allow one to locate the damage. It is claimed that the commercial AE sensor monitoring system can locate each detected wire break (to within 500 mm) [12]. Unfortunately, acoustic emission is susceptible to external noise sources interfering with the originating signal. This makes it more difficult to process and extract the waveform emitted by the damage.

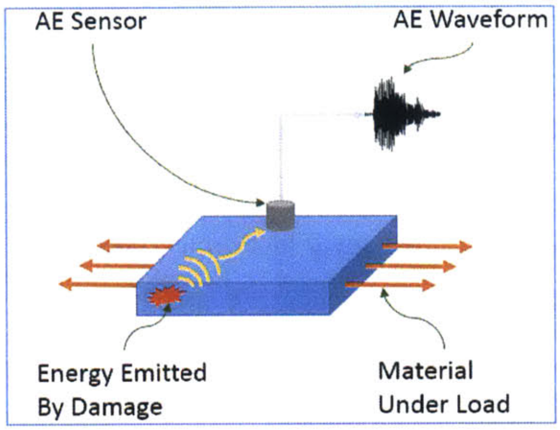

Figure 5: Passive Acoustic Emission Corrosion and Crack Detection Schematic

Another way to determine cracking is to measure the impedance of the structure. Park *et al* have demonstrated the use of micro-fiber composite patches (similar material to piezoelectric patches) to detect damage in steel beams, concrete structures, and loose bolts in aluminum [15], [16].

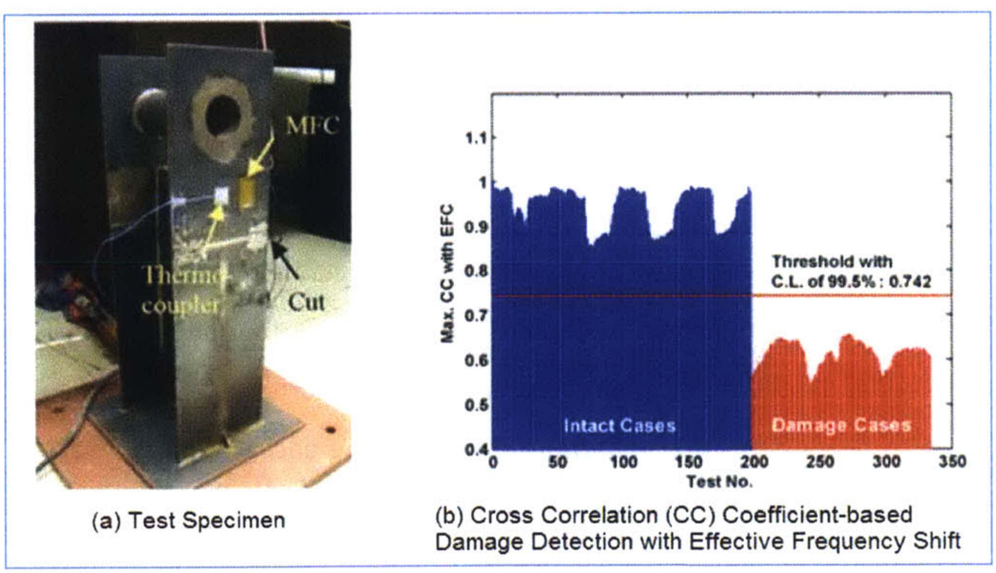

Figure 6: Results of Impedance Based Crack Determination on Steel I-Beam [15]

Micro-fiber composite patches and more traditional piezoelectric patches, will emit a voltage when perturbed or will deform when a voltage is applied. This ability to both sense and actuate is very useful for measurements and it is cost effective. For SHM uses, application of a waveform with only few volts peak to peak is sufficient to determine the impedance. By sweeping over a frequency range (30kHz-130kHz for example) and measuring the response it is possible to calculate the complex impedance (both the real and imaginary values) of the structure under test. Park *et al* experimentally verified that a correctly bonded piezoelectric patch will mirror the impedance of the structure to which it is bonded [17]. Within the laboratory, an impedance analyzer is regularly used to calculate the impedance response. This is a bulky and expensive piece of equipment. However, with the introduction in 2005 by Analog Devices Inc. of a 12 Bit Impedance Converter Network Analyzer integrated circuit, the AD5933, it is possible to embed this IC into sensor nodes [18]. It opens up the possibility of low cost, scalable corrosion and crack detection.

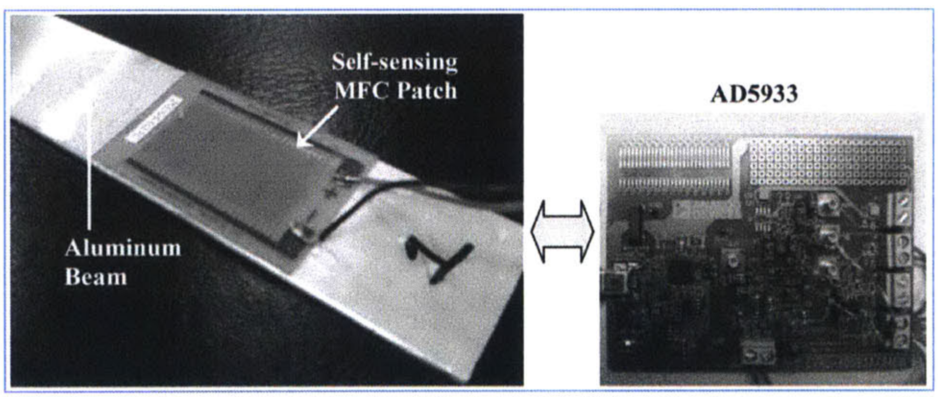

Figure 7: Self Sensing MFC Patch connected to the AD5933 Impedance to Digital Converter [19]

Corrosion

Corrosion is an important parameter to monitor as it affects many structures especially those constructed from steel or reinforced concrete. For reinforced concrete, it is also difficult to inspect as the rebar is encased in concrete and may be corroding without any perceptible indications due to deicing or other materials infiltrating the encasement. Corrosion causes the loss of reinforcement area, loss of bond between reinforcement and concrete, crack and spalling occurrence, crack propagation, and excessive deformation [19]. For steel and concrete rebar, corrosion causes the individual strands of the steel cables within a structure to crack or break.

These events will emit an energy wave. As with cracking, these acoustic emissions can be detected using piezoelectric transducers.

Figure 8: Corrosion of pre-stressing tendons within Hammersmith Flyover, London [12]

Another way to determine corrosion is to measure the impedance of the structure. Park *et al* have demonstrated the use of micro-fiber composite patches to detect corrosion in aluminum structures [20]. In other cases, the impedance of a reference piece of steel is measured as a proxy for the actual steel in the structure. As the reference material is smaller it will fail sooner, providing an early warning of structural deficiencies.

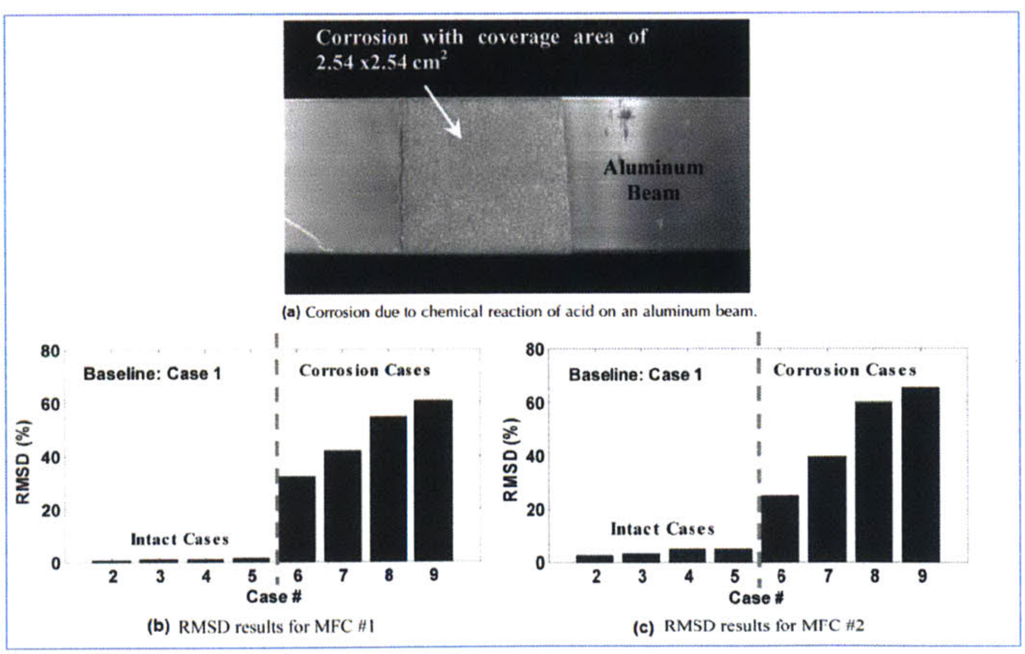

Figure 9: Results of Impedance Based Corrosion Determination on Aluminum [20]

Displacement

Local displacement such as crack length and global displacements such as deflections are important parameters to measure to determine the overall condition of a bridge [14]. For local displacement measurements transducers like Linear Variable Differential Transformers (LVDTs), Joint Meters, and Linear Potentiometers are used. For global displacement measurements equipment utilizing Global Positioning Systems (GPSs), Laser Scanning, and Photographic devices can be used.

For this analysis, we are mainly interested in measuring local facets of a structure and so we will focus on the LVDT sensor to measure displacement. The LVDT converts a position or linear displacement from a mechanical reference (zero, or null position) into a proportional electrical signal containing phase (for direction) and amplitude (for distance) information [21]. The LVDT relies on electromagnetic coupling between the moving part and a coil housed within the sensor body to generate the proportional electrical signal. As it does not contain any electronics, it can operate from -150˚C to 650˚C [21].

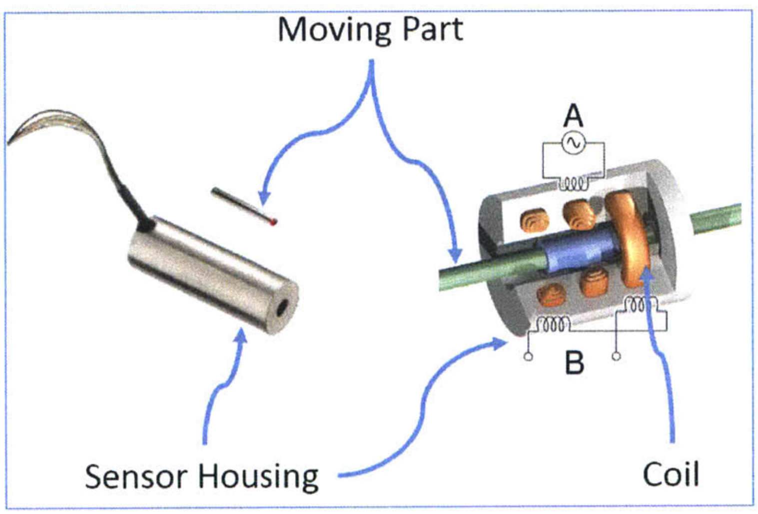

Figure 10: LVDT Sensor [22] and cross-section [21]

Strain

A material fails when the stress at a certain point exceeds the strength of material and strain is a parameter directly correlated to stress [23]. By monitoring the strain changes in structures, the factors that would cause it to fail, e.g., excessive loading and cracking, can be detected [14]. There are several ways to measure strain including fiber optics and semiconductor strain gauges. However, the most common and least expensive way is to use a foil strain gauge. A foil strain gauge is made from a metal that change resistance as it is strained. This change in resistance is linearly related to the strain causing the deformation of the gauge. It is susceptible to temperature and environmental noise.

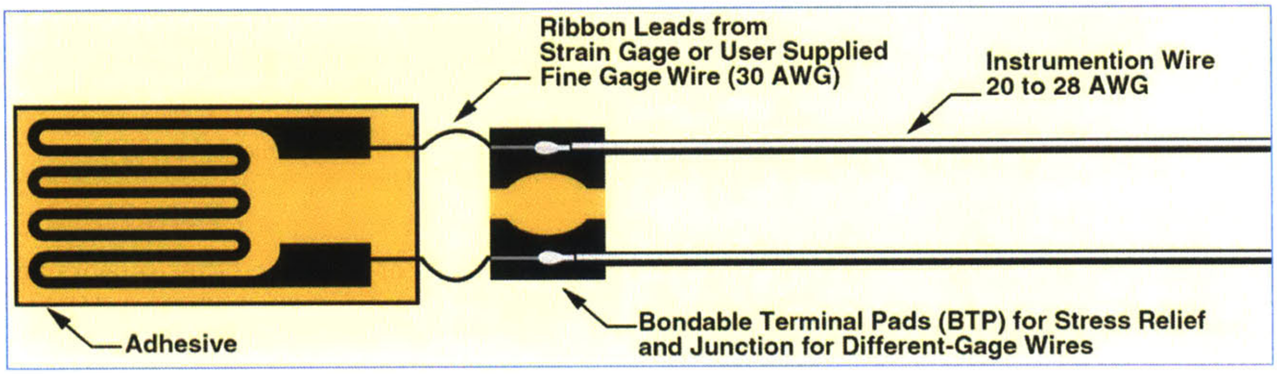

Figure 11: Foil Strain Gauge [24]

Vibration

Bridges experience extreme vibrations, particularly in the cases of passing trucks, and thus the vibration is another vital parameter to monitor [14]. Accelerometers measure these vibrations, mostly < 10Hz, and over time it is possible to use this data to construct a model of how the bridge deforms over time. When this information is combined with traffic and temperature it is possible to determine the effects of these external events on the structure. Accelerometers also provide details of any seismic events and they can quickly indicate if a seismic event displaced the structure in any way. Such information may allow the structure's owner to quickly determine if the structure can return to use after an earthquake.

Common types of accelerometers are piezoelectric and capacitive. However, for sensor nodes on bridges, the most commonly used accelerometer is the micro-machined electro-mechanical (MEMS) capacitive accelerometer. It contains a movable mass sandwiched between two springs. The mass (or plate) moves when subjected to acceleration. The mass also has fingers which protrude out from the main body. Each finger sits between two fixed outer plates. The integrated circuit measures the capacitances between the two fixed outer plates and the finger attached to the mass. This allows the circuit to determine acceleration value and direction.

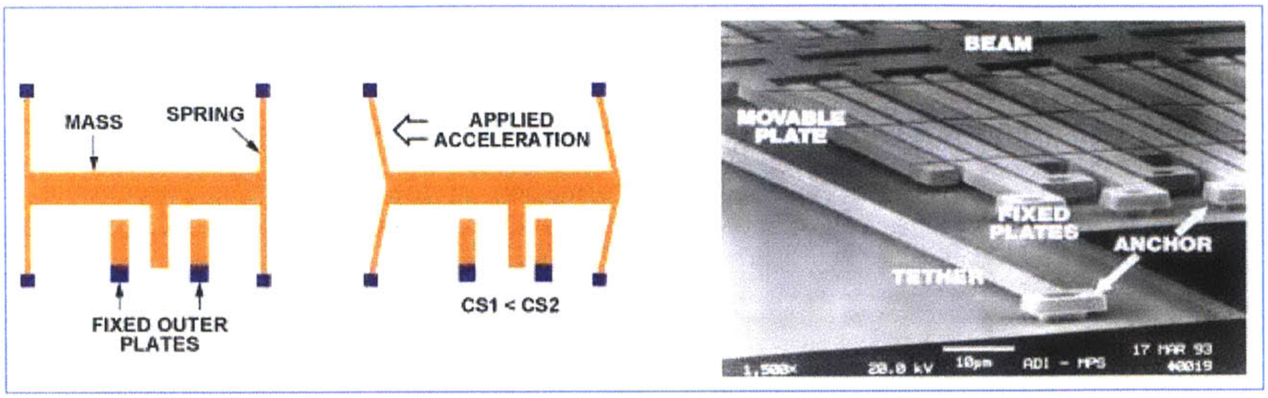

Figure 12: Capacitive Accelerometer Diagram and Scanning Electron Microscope Image of portion of ADXL50 [24]

Temperature & Humidity

Temperature and humidity are external environmental sources of error for other sensors and they can have significant impact on the structure itself. Measuring these values over time is critical however they do not need to be measured on a local basis, a global perspective across the structure should be sufficient. It is possible to measure temperature using thermocouples (a temperature change generates a minute voltage different across a bi-metallic junction), thermistors (the resistance of the material changes with temperature), and fiber optics (a laser excites phosphor to luminescence and the decay rate is dependent on temperature [25]) amongst others. Humidity can be measured using capacitive humidity sensors, thermal conductivity humidity sensors, or resistive humidity sensors [26]. It is also possible to purchase sensors with both temperature and humidity integrated in one electronic device [27].

Architecture of a Wireless Sensor Node

Historically, structural health monitoring networks resembled a hub and spoke type network with each sensor connected over a dedicated cable (the spoke) to a central processing unit (the hub). The long cables were expensive to install, they were susceptible to noise, and they were difficult to maintain (a break in a cable was usually very difficult to find). Over time, the cables were shortened by connecting the sensors to a gateway which in turn was connected to a hub via wireless technology. This reduced costs but did not greatly mitigate the performance issues. Within the last 15 years, there has been a steady shift to wirelessly connected sensor nodes. This reduces installation and maintenance costs and makes the nodes more resilient to external noise and breakages. This evolution has also allowed more data to be processed closer to the nodes and only the necessary information to be transmitted back to the hub.

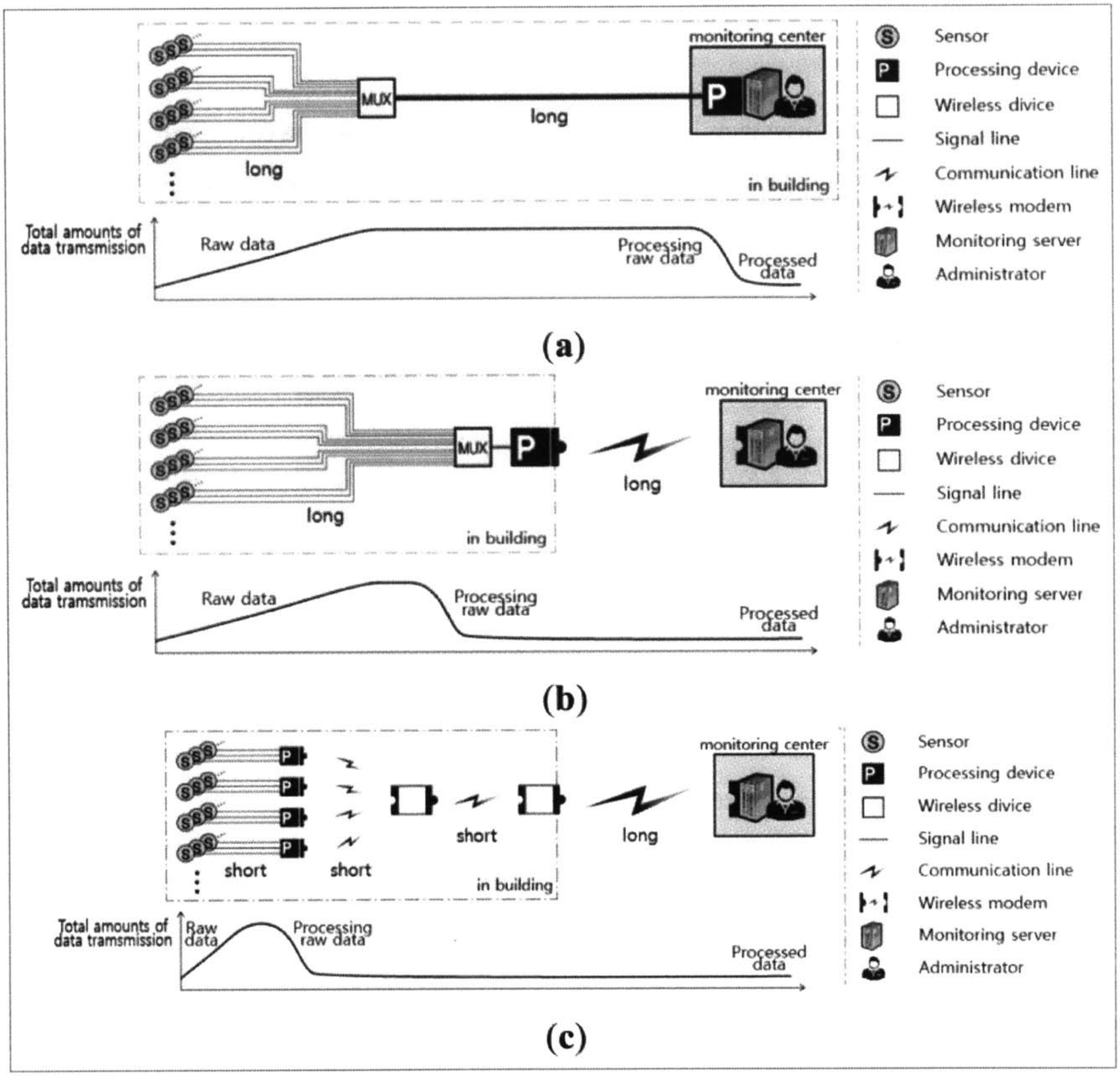

Figure 13: (a) Wired Sensor Network, (b) Hybrid Wired and Wireless Sensor Network; (c) Wireless Sensor Network [28]

According to Lynch [6], the wireless sensing unit represents the fundamental building block from which wireless structural monitoring systems for civil structures can be constructed and within a wireless structural monitoring system, each wireless sensing unit will be responsible for three tasks:

1. Collection of structural response data
2. Local interrogation of collected measurement data
3. Wireless communication of response data or analysis results to a wireless network which comprises other wireless sensing units.

These 3 tasks map to 3 subsystems within a wireless sensor node: (a) the data acquisition system, (b) the computational core, and (c) the wireless communications channel. A critical 4th subsystem is the power management block which can include circuit power management, energy storage devices, batteries, and energy harvesters.

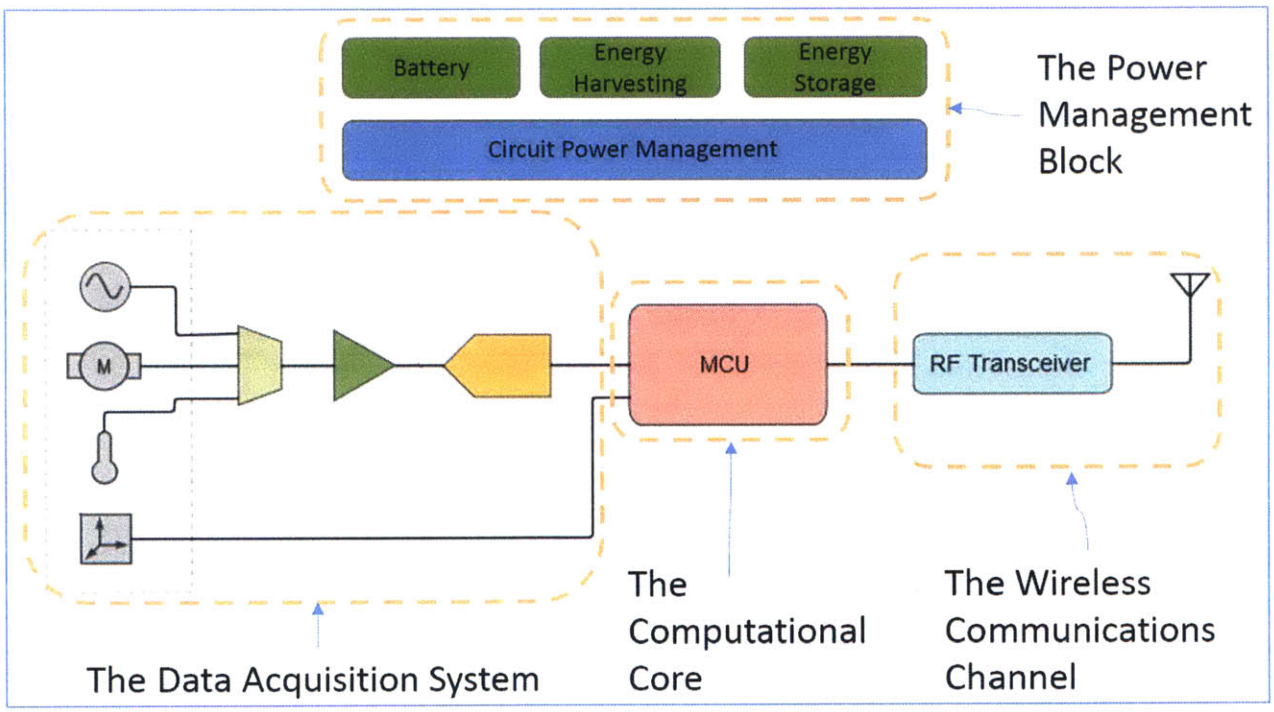

Figure 14: Generic Wireless Sensor Node Delineated by Subsystem

Data Acquisition System

The data acquisition system is made up of the sensors measuring the phenomena, a multiplexor to map many sensor inputs to a single signal conditioning path. The signal conditioning path contains an amplifier to magnify the signal and buffer the sensor from the rest of the circuit and an analog to digital converter (ADC) to digitize the signal. Many of the phenomena measured generate slow moving signals (<< 10kHz) which makes them suitable for use with Sigma-Delta ADCs. Many Sigma-Delta ADCs on the market contain all the signal conditioning required within the devices themselves. This makes it very easy to setup high accuracy measurement signal chains. Sigma-Delta ADCs regularly have accuracies greater than 16-Bits. However, if a discrete impedance measurement circuit is constructed, a higher sampling rate will be required as the frequencies of interest are above 30kHz. A successive approximation ADC is suitable to measure these signals at the requisite sampling rate (1MSPS) and accuracy (16-Bits).

functionality	design parameter	selection criteria
data acquisition subsystem	maximum sampling rate	500 Hz to 1–2 kHz
	channels	4–8 simultaneously
	resolution	at least 16 bits
	transducer types	analogue and digital sensor outputs
computational core	data storage	256 KB
	program memory	256 KB
	processing capabilities	engineering analyses (e.g. FFT)
wireless communication channel	encoding reliability	spread spectrum
	radio band	unregulated ISM bands
	open-space range	over 200 m
	data rate	at least 20 kbps

Table 2: Performance criteria for each wireless sensing unit functional module [6]

Computational Core

Not only is the microcontroller unit (MCU) the traffic cop routing digitized signals to the RF Transceiver for transmission to the central data processing center, it is also the computational brain of the wireless sensor node. In order to be this brain, it must be able to quickly compute the results of algorithms applied to floating point datasets. MCUs do not normally contain floating point processors; this meant a common MCU was very slow and consumed a lot of power when processing such algorithms. Lynch worked around this by incorporating two distinct processors, one for control and the other for algorithm processing, into early wireless sensor nodes [6]. Another alternative is to use a processor which contains a dedicated Discrete Fourier Transform (DFT) hardware block. The ADuCM350 is such a processor [29]. Recently ARM introduced a line of microcontrollers, the Cortex-M4 family, for applications "that demand an efficient, easy-to-use blend of control and signal processing capabilities" [30].

Wireless Communications Channel

The wireless communication channel must be highly reliable with little to no data loss as a result of channel interference, multi-path reflections and path losses [6]. Over the past decade several all-layer RF protocol stacks have emerged as wireless communications have taken hold. The predominant stack is called ZigBee [31]. The ZigBee Alliance publishes a set of standards which ensure all products bearing the ZigBee logo will operate together. These standards document the software and hardware requirements so that a ZigBee network is reliable, interoperable and low power. ZigBee products operate within the unlicensed (but not unregulated) Industrial, Scientific, and Medical (ISM) bands. It uses 2.4GHz across the globe and it can also use 868MHz in Europe or 915MHz in the US. It has a maximum data rate of 250kbps and a nominal range of 75 meters.

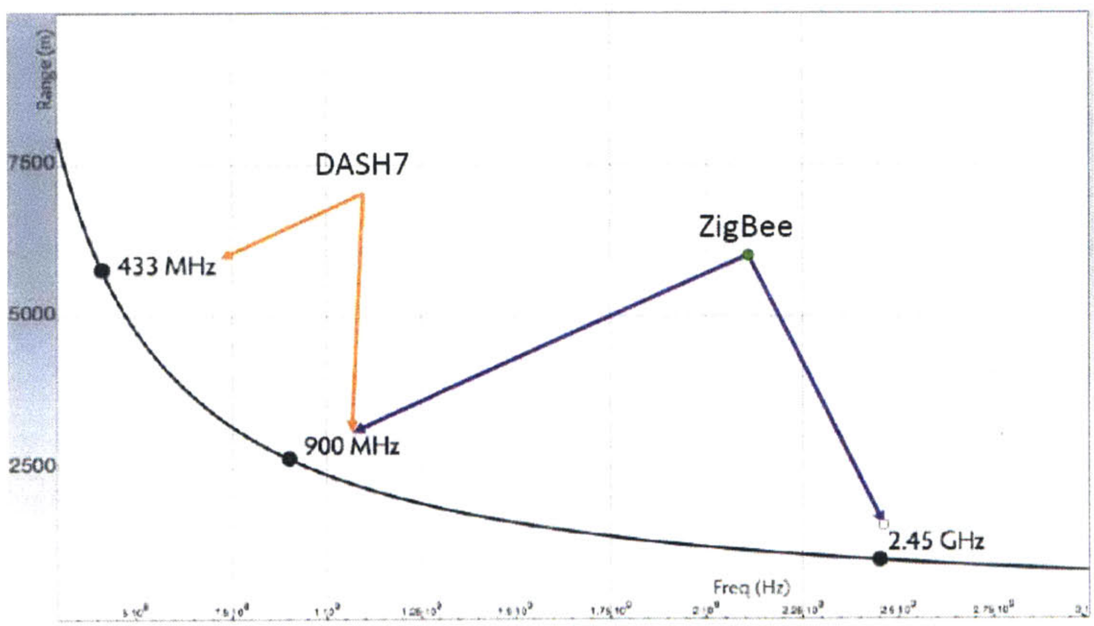

Table 3: Possible Range versus Frequency of Operation [32]

Another standard comes from the DASH7 Alliance which utilizes the ISM bands of 433MHz, 868MHz, and 915MHz. It originally had a data rate of 28kbps but it has since been increased to 200kbps. Because of its lower operating frequency, its nominal range is much longer at 250 meters [33]. However, DASH7 is not as popular as ZigBee even though it was design specifically for SHM type sensor nodes. Both standards support a star network formation. ZigBee supports a true mesh network with thousands of nodes while DASH7 instead provides for a 2-layer network to simplify the standards requirements.

SYSTEM SPECIFICATIONS		
Currents		**Example Duty Cycle**
Processor		
Current (full operation)	8 **mA**	1
Current sleep	8 μA	99
Radio		
Current in receive	8 mA	0.75
Current transmit	12 mA	0.25
Current sleep	2 μA	99
Logger Memory		
Write	15 mA	0
Read	4 mA	0
Sleep	2 μA	100
Sensor Board		
Current (full operation)	5 mA	1
Current sleep	5 μA	99
Computed mA-hr used each hour		
Processor		0.0879
Radio		0.0920
Logger Memory		0.0020
Sensor Board		0.0550
Total current (mA-hr) used		**0.2369**
Computed battery life vs. battery size		
Battery Capacity (mA-hr)		Battery Life (months)
250		1.45
1000		5.78
3000		17.35

Table 4: Battery life estimation for a senor node operating at 1% duty cycle Crossbow (2007) [34]

Power Management

Given the many inaccessible places a wireless sensor node may be placed on a bridge, it is crucial that the life of the node stretch to 10 years at least. In order to do this a combination of low power consumption, battery life, energy harvesting, and optimized duty cycling is required.

As noted in Table 4, a sensor node optimized for duty cycle of 99% off and 1% on will have a life of 17 months when running on a 3000mAh battery pack. This is not sufficient to operate a wireless sensor node autonomously for a decade. Tan and Panda recommend 3 ways to maximize operational life by tuning the power consumption or energy sources [34]:

1. Improve the performance of the finite power sources for e.g. by increasing the energy density of the power sources
2. Reduce the power consumption at different levels of the sensor nodes hierarchy i.e. signal processing algorithms, operating system, network protocols and integrated circuits
3. Develop energy harvesting techniques that enable a sensor node to generate its own power by harvesting energy from the ambient

Recommendation 1 will be constrained by the volume available to hold the wireless sensor node. If there is no space constraint, a 26,000mAh lantern style battery could be used. If it is space constrained e.g. embedded into the pavement, a coin cell battery with only 500mAh of capacity may be available.

Recommendation 2 is made up of two sub-recommendations: (a) keep the node asleep for as long as possible and (b) when asleep leak as little power as possible. Current leakage of tens of microamperes accumulate over a decade, such leakage can dramatically shorten the operational life of a node.

Recommendation 3 presents many potential options in terms of the types of energy harvesting available. What form this energy harvesting takes will be dependent on what natural resources are available to harvest. There are many possible resources available (Figure 15) but for this discussion we will examine Photo Voltaic (PV), Piezoelectric, RF, Thermoelectric and DC Rotary Generator.

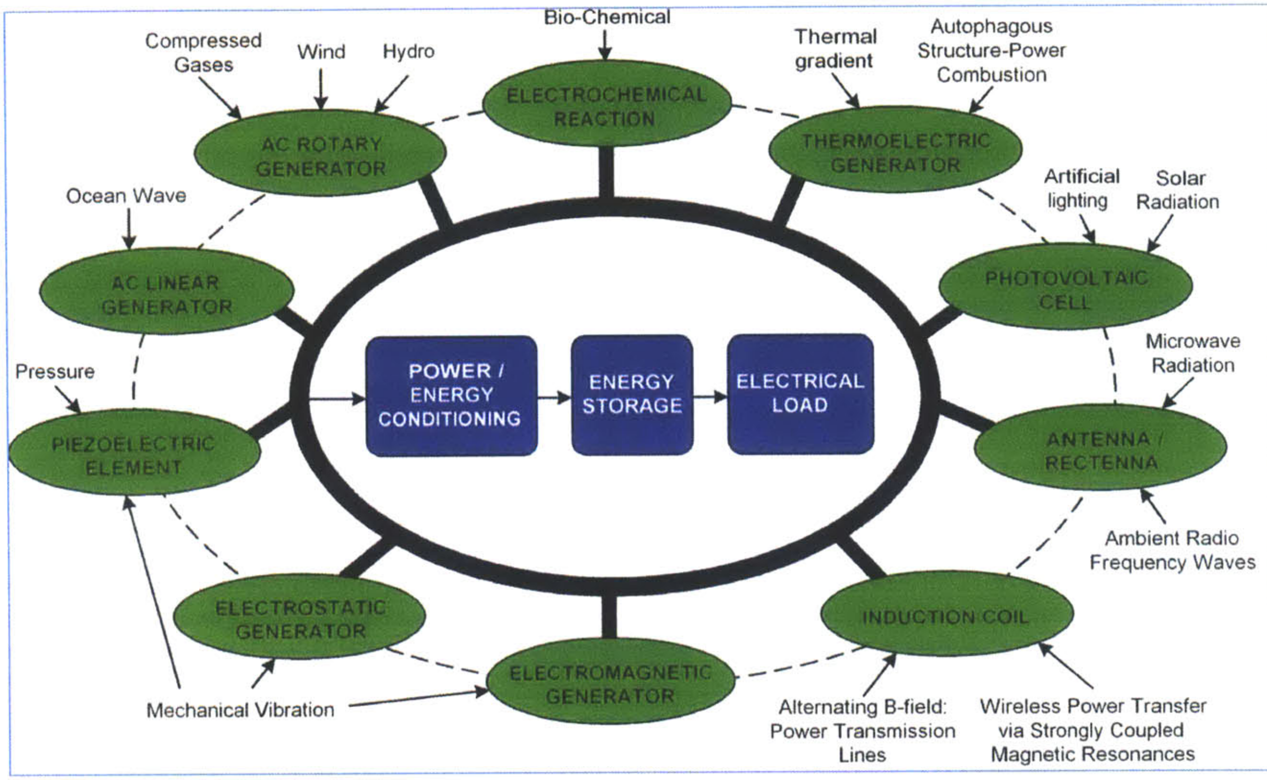

Figure 15: Energy sources and respective transducers to power autonomous sensor nodes [34]

Tan and Panda enumerated the benefits of energy harvesting for wireless sensor nodes [34]:

- Reduce the dependency on battery power. With the advancement of microelectronics technology, the power consumption of the sensor nodes are getting lesser and lesser, hence harvested ambient/environmental energy may be sufficient to eliminate battery completely.
- Reduce installation cost. Self-powered wireless sensor nodes do not require power cables wiring and conduits, hence they are very easy to install and they also reduce the heavy installation cost.
- Reduce maintenance cost. Energy harvesting allows for the sensor nodes to function unattended once deployed and eliminates service visits to replace batteries.
- Provide sensing and actuation capabilities in hard-to-access hazardous environments on a continuous basis.

- Provide long-term solutions. A reliable self-powered sensor node will remain functional virtually as long as the ambient energy is available. Self-powered sensor nodes are perfectly suited for long-term applications looking at decades of monitoring.
- Reduce environmental impact. Energy harvesting can eliminate the need for millions on batteries and energy costs of battery replacements.

For energy harvesting to be effective, the power generated must be greater than the power consumed. On an instantaneous basis it is unlikely that the harvested energy will be greater than the power consumed by the wireless sensor node will active. However, most harvested energy sources operate continuously which enables them to charge up a storage device like a super-capacitor. The energy storage device can then become the primary power source as long as the energy harvester has time to charge the storage device while the sensor node is asleep.

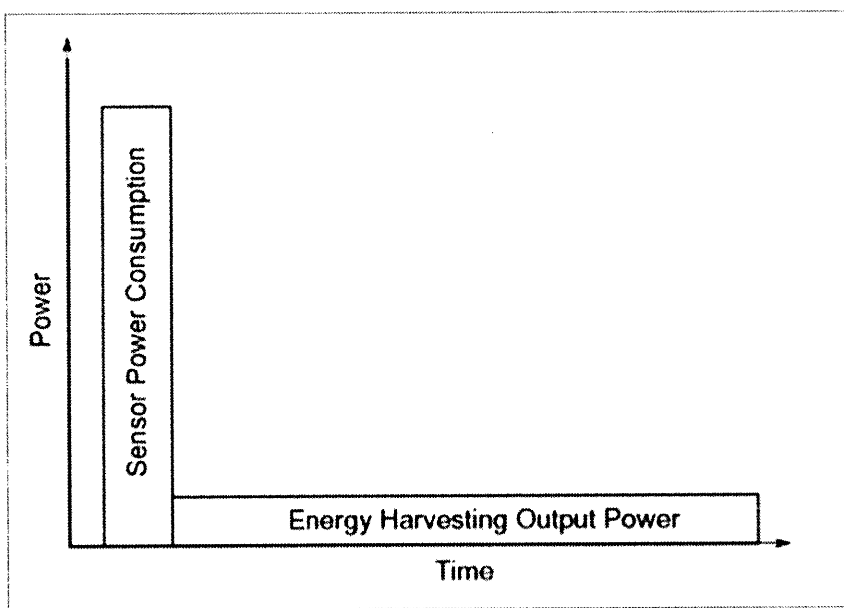

Figure 16: Energy profile of a sensor and an energy harvester over time. Adapted from [35]

Solar

Solar energy harvesting is a mature technology with wide ranging deployments. It is possible to harness solar energy both indoors and outdoors using Photo Voltaic (PV) cells. Products are available that are optimized for different lighting conditions in order to maximize the power generated. In order to increase efficiency, a maximum power point tracking (MPPT) circuit is required.

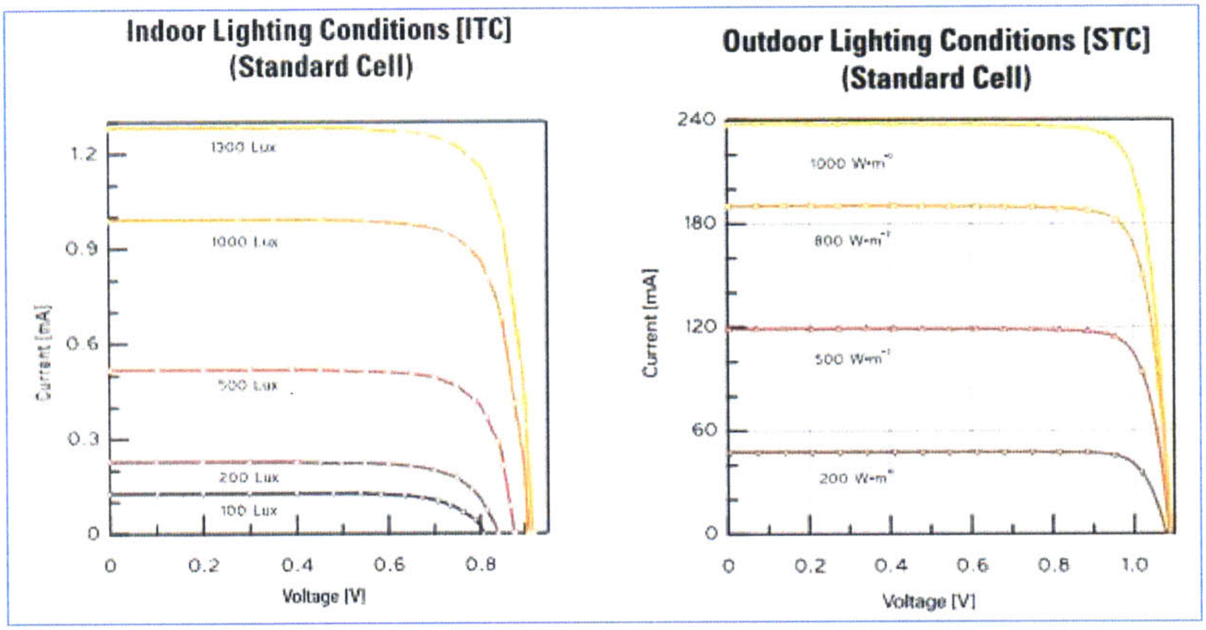

Figure 17: Performance of a single Alta Devices PV Cell in indoor and outdoor conditions [37]

Piezoelectric

As noted earlier piezoelectric transducers generate a voltage when they are perturbed. This is the basis of a piezoelectric energy harvester. It relies on vibrations in the structure it is attached to in order to generate an output voltage.

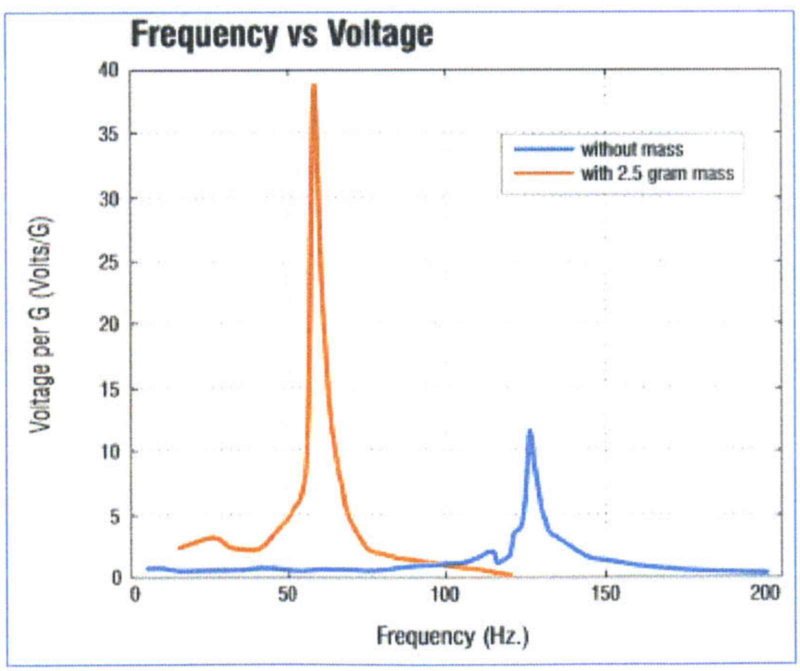

Figure 18: Chart showing the tuned nature of the Mide QPK-1001 [36]

For rotating equipment or railway cars bouncing on a track or trucks driving over a bridge, there are enough vibrations to generate enough energy for a wireless sensor network. The drawback of a piezoelectric energy harvester is that it must be tuned to a frequency in order to maximize the amount of power generated. This can narrow its applicability especially in structures like bridges where the frequency of vibration is very low and will change depending on temperature and traffic.

RF

Harvesting RF energy from ambient sources such as TV, Cellular Telephony, and Wireless LAN base stations sounds very promising as these signals are omnipresent in urban environments and open the possibility to realize truly autonomous wireless sensors but unfortunately, this is only feasible for a limited number of applications as the available power generally is very low and unreliable [35]. Ambient RF energy induces an electric charge in an antenna. This electric charge is accumulated and converted into a DC output. To maximize output and ensure the greatest power conversion efficiency, the RF energy harvester must be tuned to a specific frequency e.g. 915MHz.

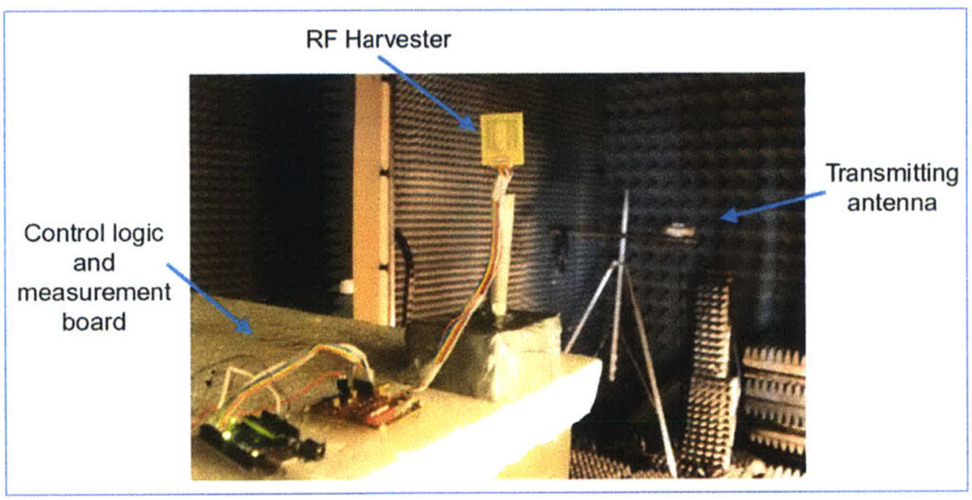

Figure 19: Measurement setup of RF Energy Harvester in anechoic chamber [35]

Thermoelectric Generator

A thermoelectric generator converts a temperature gradient into electrical energy. A simple thermoelectric generator can be created by connecting thermocouples in series. A bi-metallic thermocouple will generate a small voltage across its junction. The magnitude of the voltage is proportional to the ambient temperature. Most of the thermoelectric generators to be used at room temperature employ bismuth telluride and have a Seebeck coefficient around 40 mV/K to 100 mV/K [37]. At room temperature gradient of at least 5°C (preferably 10°C) is required to generate a voltage from a thermoelectric generator.

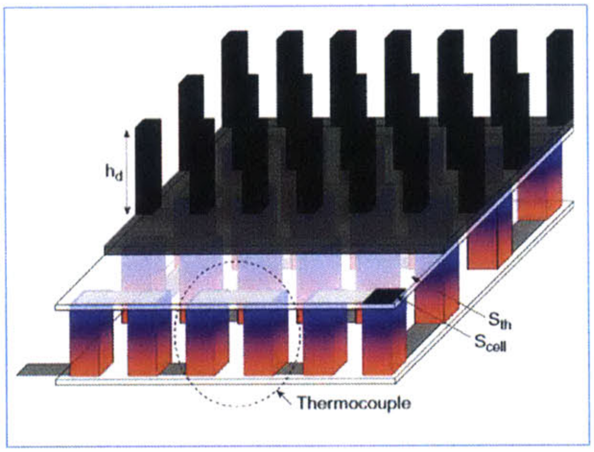

Figure 20: Physical Structure of a Thermoelectric Generator

DC Rotary Generator

Another name for a DC Rotary Generator is a small DC wind turbine. Bigger versions are available with AC generators. Most wind turbines have a minimum air speed requirement before they begin to generate electricity. In most cases it is at least 4mph (2m/s). This would be considered a light breeze on the Beaufort scale. It is also within the lower bounds of wind speeds recorded in Boston.

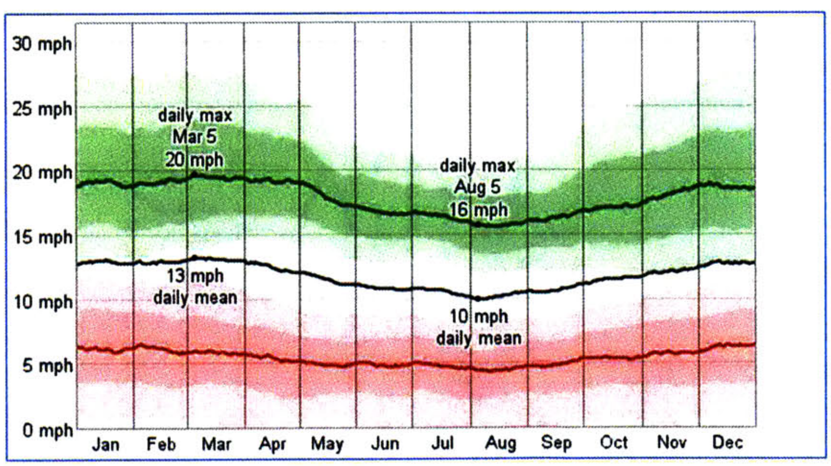

Figure 21: Average Daily Wind speeds in Boston [38]

Another consideration for wind turbine is selection of architecture: horizontal or vertical. A horizontal wind turbine is the traditional form with blades which spin and a tail which rotates the unit to keep in facing the wind. A vertical wind turbine has blades in the shape of a helix which are mounted vertically. It does not require a tail fin as it will work with any wind direction. It can also be more compact in size.

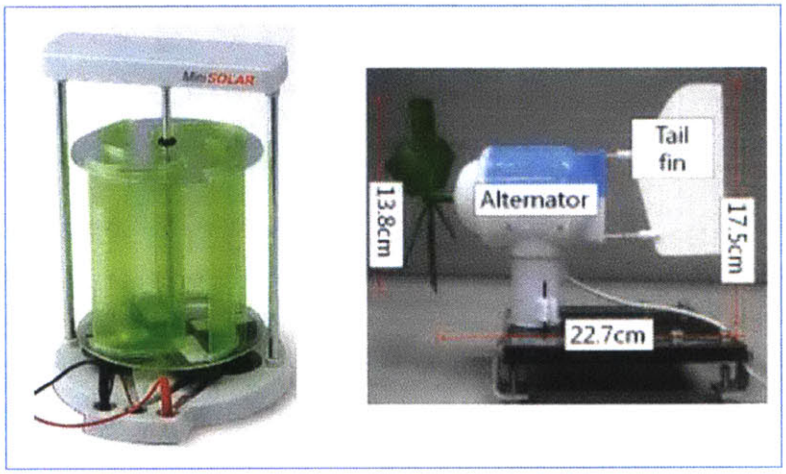

Figure 22: Vertical [39] and Horizontal Wind Turbines [7]

Maximum Power Point Tracking

Many energy harvesters "have an internal parasitic ohmic resistance, it is useful to think about matching the load to this resistance in order to get the maximum power out" of the energy harvester [37]. By matching the output load on an energy harvester, the efficiency of the system can be maximized. Products like the ADP5090 automatically adjust the output load on the energy harvester so the super-capacitor or rechargeable battery can get the most current available.

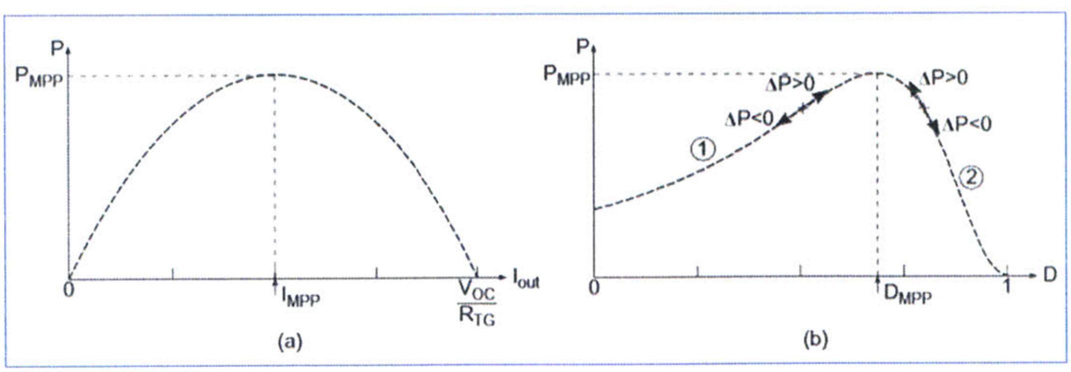

Figure 23: Matching a load to an energy harvester: Output power versus (a) output current and (b) duty cycle [39]

Multi-Attribute Tradespace Exploration

The Multi-Attribute Tradespace Exploration (MATE) framework was developed to address process limitations in the early phases of aerospace system design. Such limitations can lead to developments which exceed cost estimates, require prolonged development times, or miss critical customer requirements. Nathan Diller [40] and Adam Ross [41], while working on their graduate theses at MIT, combined Multi-Attribute Utility Analysis (MAUA) and tradespace exploration to create the MATE framework.

MATE incorporates value-focused thinking [42] which sets out the desired outcome and then works back from there to determine how to achieve it. This is in contrast to alternative-focused thinking which evaluates known solutions and selects the best solution from that list. By utilizing value-focused thinking, MATE increases the likelihood a solution will perform well in value and it allows for exploration of novel solutions that may not have been discovered by the alternative-focused process. Each stakeholder will wish to extract value from the system under design. This value can be mapped to attributes of the system through utility functions. In this way, alternative implementations of the system can be scored based on the attributes which in turn translates to how well or poorly the implementations meet the desired value of the stakeholders. This ability to compare different and disparate implementations allows one to greatly expand the potential solution space, enabling the designer to break-free of existing or anchored solutions.

Additionally, a tradespace [43]:

- Enables model-based high-level assessment of system capability
- Allows many designs to be assessed
- Avoids optimized point solutions
- Provides a way to assess the value of potential capabilities

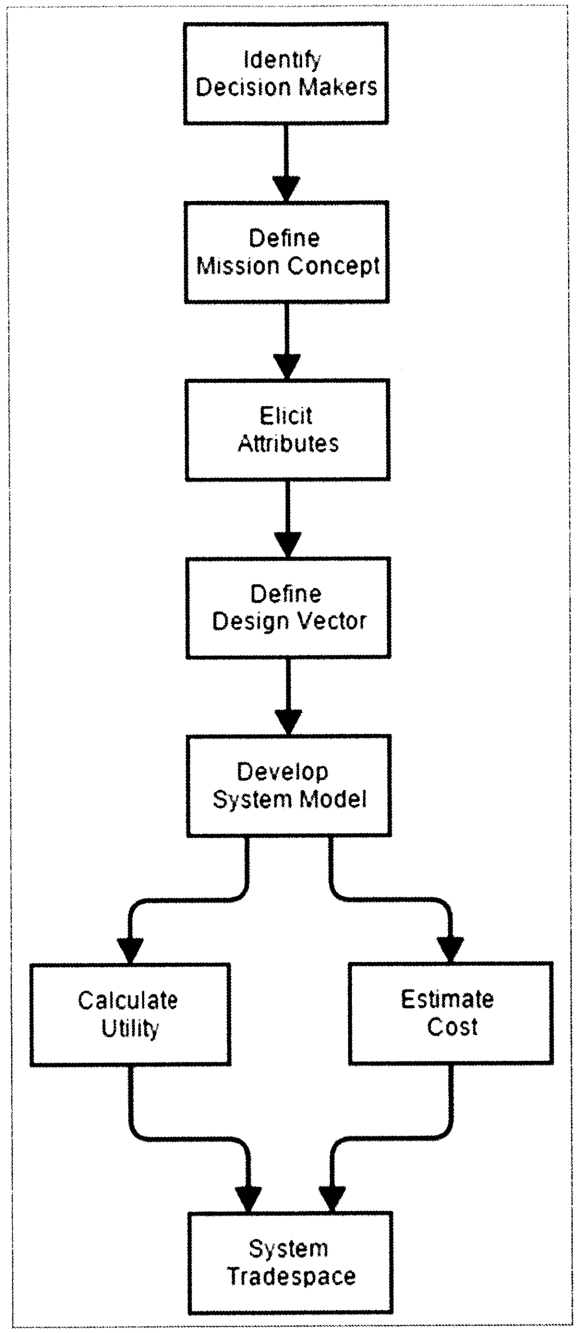

Figure 24: Simplified MATE Process Flow

For clarity, I will utilize the following definitions which are taken from Ross [41]:

- Attribute: a decision maker-perceived metric that measures how well a decision maker-defined objective is met
- Concept: a product or system vision, idea, notion, or mental image which maps function to form and embodies "working principles"

- Tradespace: the space spanned by completely enumerated design variables. It is the potential solution space
- Utility: a dimensionless parameter that reflects the "perceived value under uncertainty" of an attribute
- Value: a preference measure that captures the ordered ranking of bundles over all outcomes

An optimized set of steps for the MATE framework were enumerated in Ross' thesis [41]. The original list contained 48 individual steps through 7 stages and 5 phases. For the purposes of this exploration, I will use the steps outlined in the short course by Ross & Rhodes "Value-driven Tradespace Exploration for System Design" available on the Systems Engineering Advancement Research Initiative website [43].

Step 1 – Determine Key Decision Makers

According to Ross & Rhodes, a "decision maker is a stakeholder with significant influence/control over resources and/or driving needs" [45]. In an ideal situation there would be one decision maker, a dictator in essence, who has the main say in selecting the system. However, in most situations more than one decision maker will be discovered. Identifying the correct decision makers is critical to ensure success. Bridges span local, state, and federal jurisdictions and they intersect many communities which all contribute to a potentially large set of stakeholders and a significant number of decision makers.

Federal Highway Administration		MassDOT	
Bridges & Structures	Research Organization	Highway Administration	
Office Director	Office Director	Research & Materials	Bridge
Structural Engineering	Infrastructure Analysis		Operations
Structures Management	Pavement Performance		Project Development
	Infrastructure Management		

Contractors	City Organizations	
Construction Companies	Department of Public Works	City Government

IT and Systems Integrators	Construction Management	Mayor
Structural Health Monitoring Equipment Vendors		Councilors

Metropolitan Area Planning Council	Regional Transportation Advisory Council
Neighborhood Community Organizations	Environmental Organizations

Table 5: Sample List of Potential Stakeholders and Decision Makers for Bridges in Boston

Due to time constraints it was decided to forgo discovery of stakeholder needs in favor of determining needs from existing SHM literature.

Step 2 – Scope and Bound the Mission

The mission is to measure both local and global phenomena in order to determine the structure health of a bridge. The scope of this exploration is to examine wireless sensor node concepts which measure phenomena in different places on a bridge structure. It includes various sensors for measuring phenomena, electronic circuitry for processing and communicating the sensor reading, and power sources for the wireless sensor nodes. It does not include the connectivity from the gateway to the data aggregator nor does it include analysis of the data to determine the state of health of the structure. With scope set, two concepts were created.

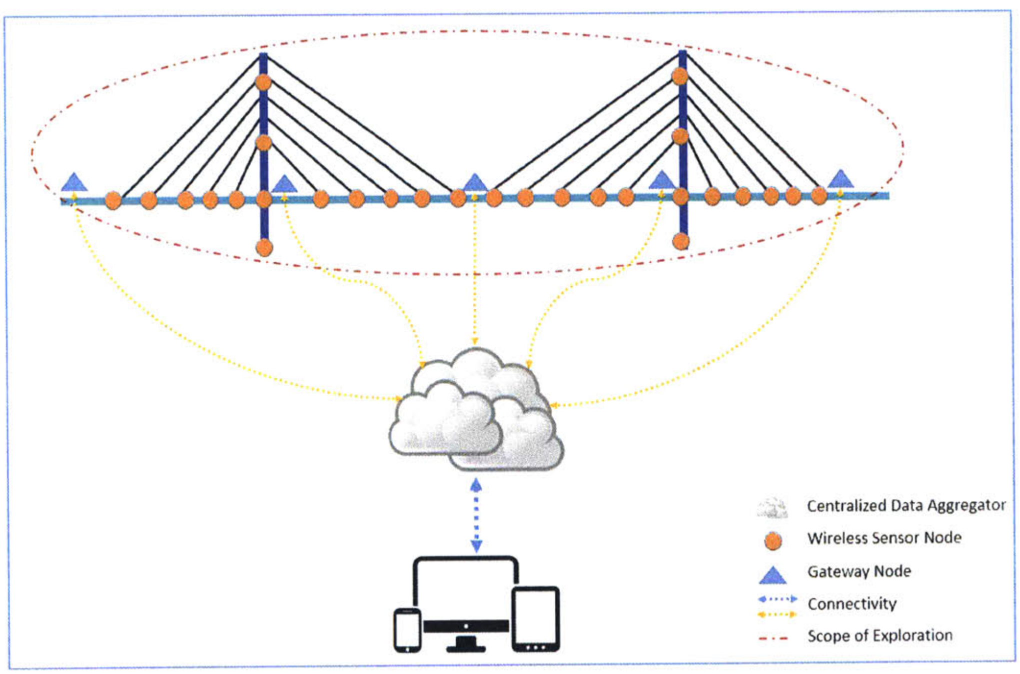

Figure 25: Scope of Exploration

Concept 1

The first concept is a discrete sensor data acquisition and signal conditioning circuit with microcontroller and RF Transceiver. This is similar to other wireless sensor nodes described in academic journals [44] [6]. The circuit allows for numerous sensors to be connected to the WSN by multiplexing the sensor inputs through the signal conditioning and digitizing circuitry of the Analog to Digital Converter. Once digitized, the microcontroller can further process the sensor readings and then transmit the data to the central data aggregator via the gateway node.

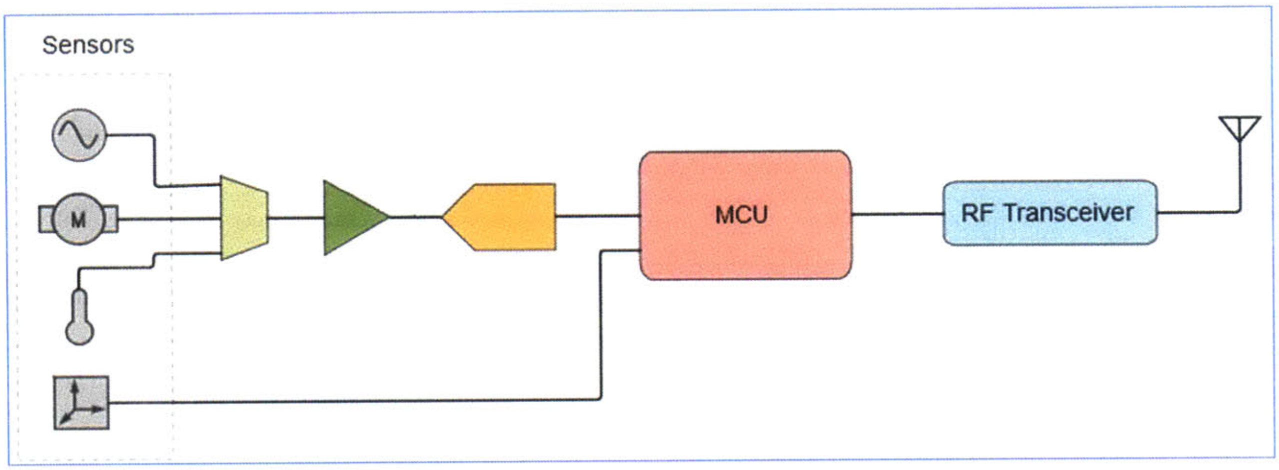

Figure 26: Generic Wireless Sensor Node Signal Chain

Concept 2

The second concept is a more integrated version of concept 1. It incorporates much more of the circuitry within 1 single integrated circuit. It also incorporates custom circuitry to process frequency based sensor readings which may yield performance improvements over the first concept. Additionally, it is possible for the sensor signal conditioning circuitry (called the Analog Front End or AFE) to be operated in an autonomous manner from the microcontroller. This allows the microcontroller to sleep while the sensor data is gathered thus reducing power consumption.

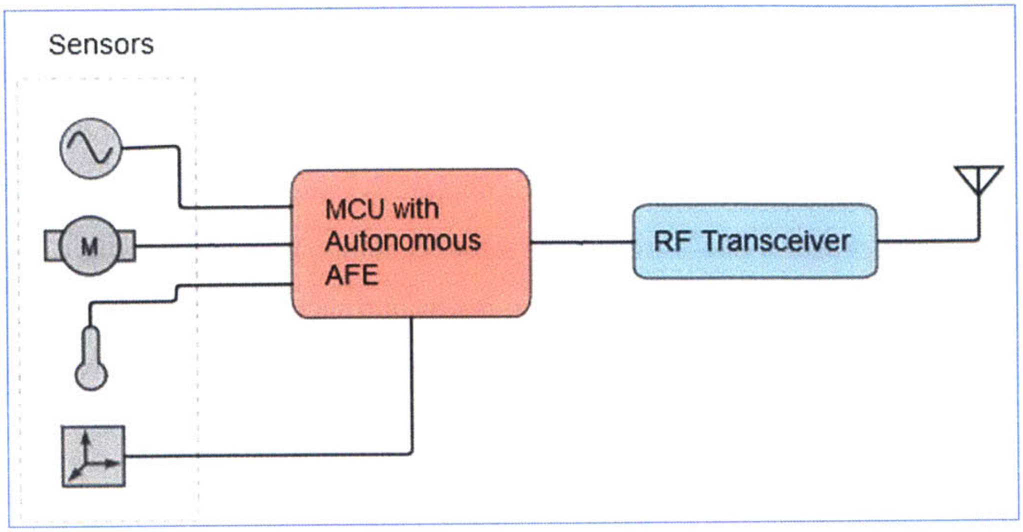

Figure 27: Integrated Wireless Sensor Node Signal Chain

Step 3 – Elicit Attributes

An attribute is "a decision maker-perceived metric that measures how well a decision maker-defined objective is met" [41]. Attributes should:

- Obey perceived independence
- Reflect what the decision maker cares about
- Be computable
- Be sensitive to design decisions

Typically, MATE uses Multi-Attribute Utility Theory (MAUT) to aggregate attributes into a "single utility selection criterion score" [43] called the Multi-Attribute Utility. However, MATE does not require MAUT as any aggregation method can be used to compress the selection criteria to a single dimension. All aggregation methods including MATE have limitations [45] [41] while biases of stakeholders contributing to the definition of the methods have significant effects.

To determine the attributes and the utility functions for each attribute, it is recommended to conduct 2 interviews per decision maker. The first interview is used to determine the most important attributes, their ranges and units of measure. The second interview is used to iteratively determine the utility function for each attribute. At the end of the two interviews, the preferred attributes, utility functions and aggregation weights will be known for each decision maker. Unfortunately, in the time allotted, it was not possible to conduct interviews with key decision makers; instead, a literature review was conducted. From this review, the attributes and the individual attribute range, unit of measure, and utility function were determined and estimated.

Attributes	Units	Best	Worst	Source	Utility Function
Operational Lifetime	Years	10	1	[46]	$U(x) = \frac{1}{1+e^{(-1*(x-5))}}$
Coverage of Structure	Sensors/m^2	1	0.1	[47]	Histogram (top = 0.3, sides = 0.2, bottom = 0.5)
Timely Updates	Updates/hour	60	1	[48]	$U(x) = \frac{1}{1+e^{(-0.15*(x-25))}}$
Types of Phenomenon	Discrete List	1.4	0.1	[14]	$U(x) = \frac{1}{1+e^{(-4*(x-0.7))}}$

Table 6: Identified Attributes, Units, Unit Range and Utility Function

Phenomenon	Utility Weight	Sensor Manufacturer	Sensor Source
Crack Detection	0.4	Smart Materials	[49]
Vibration	0.2	Analog Devices	[50]
Strain	0.2	Omega	[51]
Temperature & Humidity	0.1	Measurement Specialties	[52]
Displacement	0.2	Measurement Specialties	[53]

Table 7: Phenomena, Utility Weights, and Sensor Manufacturers

The weights in Table 7 reflect the difficulty in implementation of a sensor to measure the phenomenon. For example, Crack Detection is weighted more than Temperature and Humidity as the former requires the measurement of the impedance of the structural item under test which involves a frequency sweep, real and complex number calculations and Discrete Fourier Transform calculations while the measuring the latter is a matter of reading the digital value from the Temperature & Humidity IC. Vibration, Strain, and Displacement are also common measurements but they are a little more complex to setup.

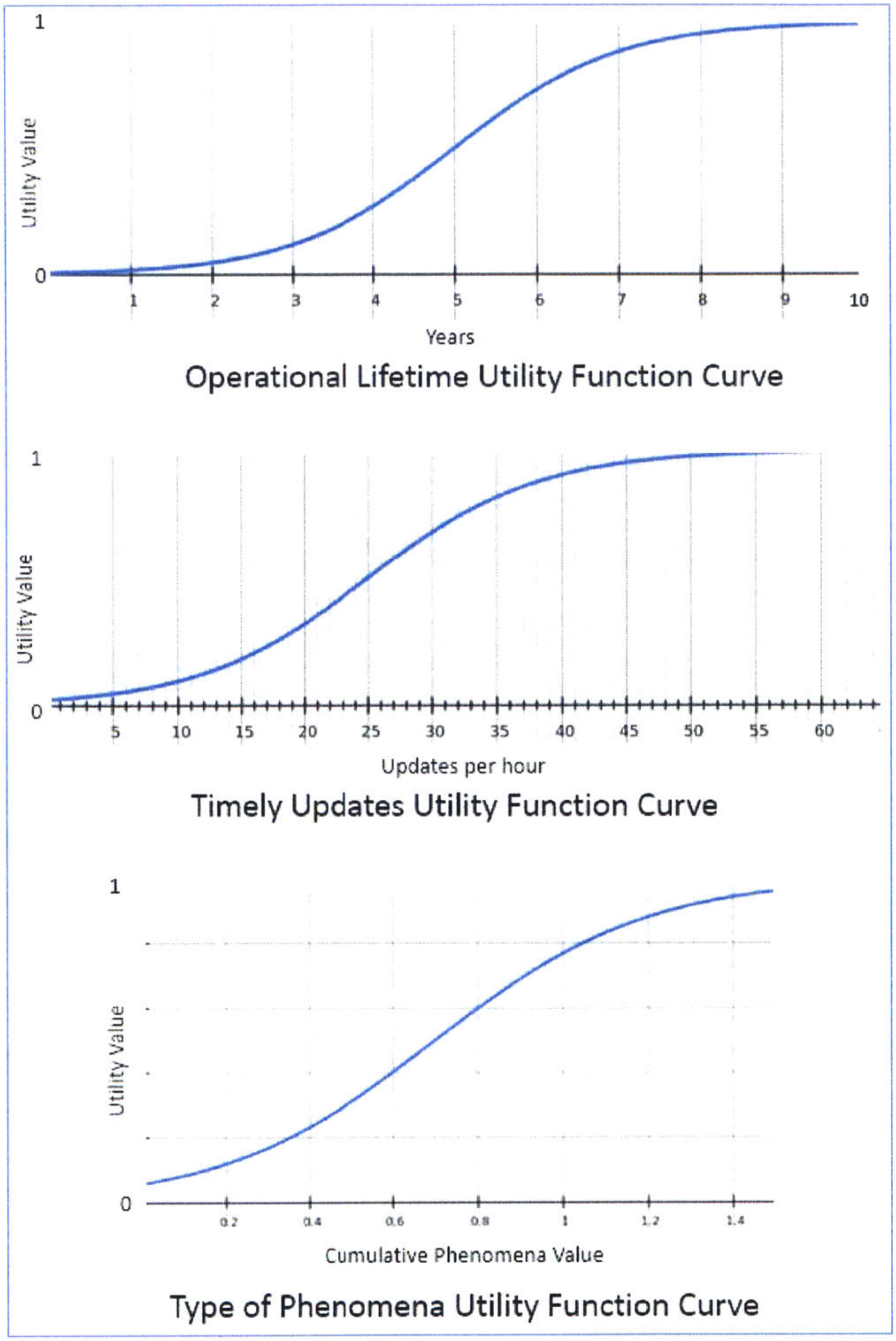

Figure 28: Utility Function Curves

One last step is to define the aggregating function. If MAUT was applied and followed as prescribed by MATE, the Keeney-Raiffa Multiplicative Utility Function [54] is recommended. It requires a series of weights which are determined during the interview process. As noted earlier, MATE does not require MAUT [43] and as the time has not been taken to elicit the attributes through the MATE recommended methods, a simple average of the individual utility functions will be used as the aggregating function. This is similar to the Keeney-Raiffa Additive Utility Function but with each utility function weighted equally:

$$U(x) = \frac{1}{n}\sum_{i=0}^{n} U_i(x_i)$$

Step 4 – Define Design Vector Elements

It is at this point the framework moves focus from the customer to the system designer. The system designer must establish a set of design variables that relate to the concepts. The design vector "defines the space of designs that will be considered" [43]. Good design vector elements as enumerated by Ross and Rhodes [43]:

- Capture the range of possible solutions
- Are realistic
- Are under the direct control of the designer
- Impact the attributes

An examination of common wireless sensor nodes found in literature [6] helped determine the key parameters that are of interest at a systems view. The initial set of design variables were determined to be:

- Type of Sensor
- Power Source
- Algorithm Usage
- Number of Channels
- RF Network Design

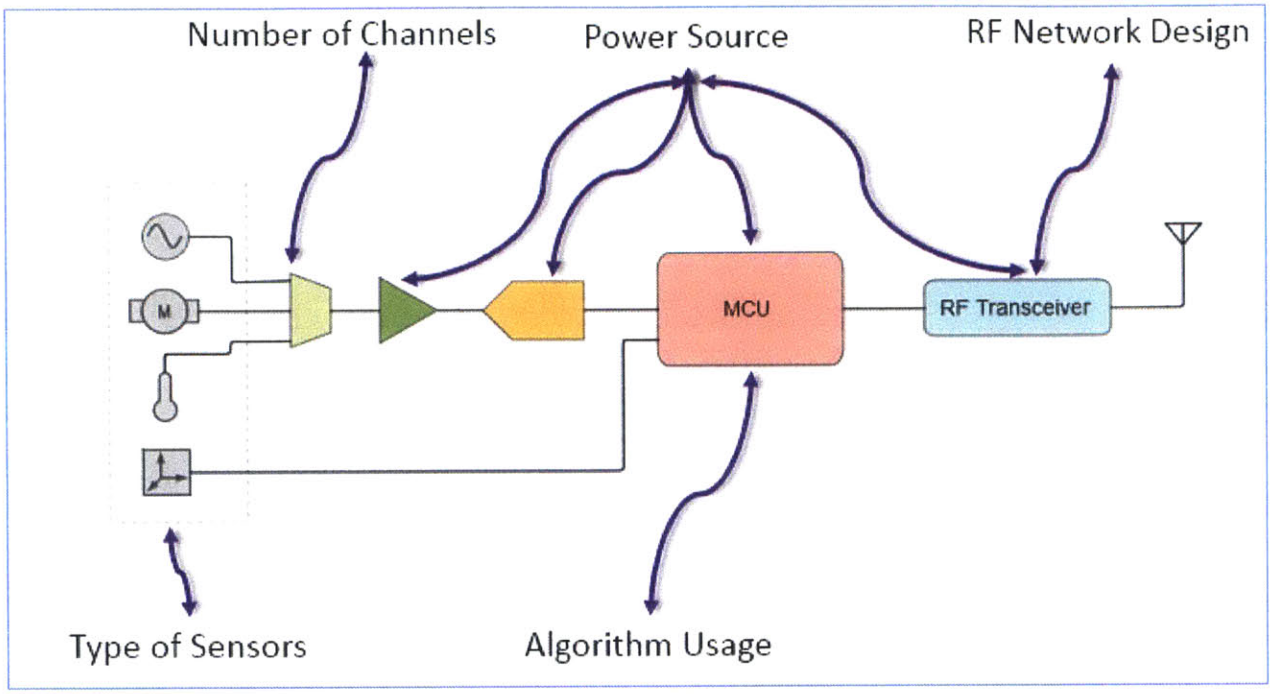

Figure 29: Areas of Impact of Attributes as mapped to generic wireless sensor node system

Listed below, in a series of tables, are the design variables with their key parameters. Table 8 contains list of sensors and the phenomena they measure. It also provides a list of sample of sensor manufacturers and associated part numbers.

Sensor	Phenomenon Measured	Sample Manufacturer	Sample Manufacturers Part Number	Source
Piezoelectric	Corrosion & Crack Detection	Smart Materials	Micro Fiber Composite	[49]
Accelerometer	Vibration	Analog Devices	ADXL362	[50]
Strain Gauge	Strain	Omega	SGD Series	[51]
Temperature & Humidity	Temperature & Humidity	Sensirion	SHT21	[27]
LVDT	Displacement	Measurement Specialties	E Series	[53]

Table 8: Sensor List

Table 9 details the 4 energy harvesting sources that were selected based on the availability of commercial solutions. It provides 3 typical current supply values and the daily hours of operation of the energy source. The Photovoltaic (PV) cell is a staple of wireless sensor nodes. However, due to the concerns on performance of PV cells in a 2012 paper by Park *et al* [7], it was decided to incorporate several other energy sources as options into the design. Park *et al* found that the voltages on batteries recharged by solar under the bridge deck were slowly decreasing while those batteries above deck on cables maintained their charge. It also became necessary to determine the hours of operation per day for each energy source. This allowed for a better system model; more of which will be discussed in Step 5.

Energy Source	Low (mA)	Med (mA)	High (mA)	Hours of Operation	Source
Wind Turbine	2	4	6	6pm-7am	[55], [7]
Piezo Electric	0.24	0.6	5	6am-10am, 3pm-7pm	[56]
Photovoltaic Cell	3	100	380	8am-4pm	[57]
RF Scavenger	0.2	2	10	6am-10am, 3pm-7pm	[58]

Table 9: Energy Harvesters and associated parameters

Other sources investigated but not selected for use include Thermoelectric Generators (TEG) [59] and Hydrogen Fuel Cells [60]. The TEG required a large temperature different to generate power; without a source of heating or cooling the whole system would be at the same ambient temperature which would not enable the TEG to generate power. The hydrogen fuel cell required replenishment when the hydrogen was consumed. In effect it operated more like a rechargeable battery. This would require a maintenance cycle to refill the hydrogen canister. This was not an acceptable design choice.

Lastly, 3 electro-chemical energy sources in the form of different types of batteries were also included in the design. These were coin cell, 'AA', and lantern sized batteries with 500mAh [61], 2500mAh [62], and 26000mAh [63] capacities respectively.

Table 10 has 2 entries for competing RF Network designs. These two networks differ by operating frequency, signal range and data rate while they both support similar network topologies. ZigBee is a popular, global communications protocol standard while DASH7 is primarily found in the US and Europe due to communication regulations. DASH7 has the advantage of requiring less power and can be used over longer distances due to its lower operating frequency.

RF Network	Frequency	Range	Topology	Data Rate
DASH7	433MHz	250m	Point to Point, Star, Limited Mesh	28kbps
ZigBee	2.4GHz	75m	Point to Point, Star, Mesh	250kbps

Table 10: RF Network Design [33]

Finally, both "Algorithm Usage" and "Number of Channels" are characteristics that must be modelled as part of the circuitry represented in each of the concepts.

To determine if the design variables affect the attributes, a Design Value Matrix was constructed. This highlighted the relationship between the design vector and the attributes. The scale of impact used was: 9 (strong), 3 (some), 1 (weak), 0 (none). The "Operational Lifetime" attribute is impacted significantly by nearly all of the identified design variables as evidenced by a score of 39 out of 45. Similarly, "Timely Updates" and "Types of Phenomenon" are also impacted by a majority of the design variables.

Attributes / Design Variables	Type of Sensors	Power Source	Algorithm Usage	Number of Channels	RF Network Design	
Operational Lifetime	9	9	9	9	3	39
Coverage of Structure	1	0	0	3	3	7
Timely Updates	0	9	0	1	9	19
Types of Phenomenon	9	3	9	1	0	22
	19	21	18	14	15	

Green	Good
Yellow	Neutral
Pink	Undecided

Figure 30: Design Value Matrix

From the design value matrix it is clear the coverage of the structure has little impact on design variables. In hindsight, it is clear that the standalone nature of a wireless sensor node around which sensors are clustered contributed to this. To increase coverage of the structure, increase the number of wireless sensor nodes. This does affect the RF Network Design but only mildly as networks can easily grow to thousands of nodes, more than enough for this application. Also, it became difficult to determine how to calculate coverage of the structure as it is very dependent on the structure itself. Based on this the "Coverage of Structure" attribute was removed from the attributes list. This impacted "Number of Channels" and "RF Network Design" by dropping their scores to 11 and 12 respectively; values that are borderline but were left in all the same. With a finalized list of design variables it is possible to create the model which will link the design vector and the attributes to calculate the utility values and costs.

Step 5 – Develop Models Linking Design Vector and Attributes

In order to link the design vector to the attributes, a model of the concepts must be created. Taking each attribute individually, it is possible to determine which design variable and system parameters are used to calculate it.

Types of Phenomena

The utility of this attribute can be calculated by summing up the phenomenon weight values as assigned in Table 7. For example, if the concept only measures Temperature & Humidity (a 0.1 utility weight) and Displacement (a 0.2 utility weight), the sum is 0.3. This value would be entered into the utility function

$$U(x) = \frac{1}{1 + e^{(-4*(x-0.7))}}$$

$$U(0.3) = \frac{1}{1 + e^{(-4*(0.3-0.7))}} = 0.168$$

A table of phenomena was assembled to range from a couple of sensors to a fully loaded wireless sensor node. The number of phenomena sensed also affects the cost as the number of sensors and signal conditioning components is dependent on this number. Additional components also affect current consumption, duty cycle and battery lifetime. The total effect will be dependent on the concept in use when the calculations are made.

Temperature & Humidity	Vibration	Impedance	Displacement	Strain
1	1	0	0	0
1	1	0	0	1
1	1	0	1	0
1	1	0	1	1
1	1	1	0	0
1	1	1	0	1
1	1	1	1	0
1	1	1	1	1
1	1	2	2	2

Table 11: Number of Sensors per combination

Timely Updates

The frequency of updates can range from 1 per hour to 1 every minute. Rather than using a continuous range, a sample set of update rates was used in the model: 1 minute, 5 minutes, 30 minutes, and 60 minutes.

Operational Lifetime

This attribute is the most complex to model as it requires deep knowledge of how the system operates as a whole and how each individual component performs in multiple states of operation. In order to calculate the operational lifetime of the wireless sensor node one must calculate the lifetime of the battery. The battery's lifetime, if short, becomes the operational lifetime of the wireless sensor node. How long the battery lasts depends on how much energy is sourced from it or from the energy storage device (a super-capacitor) which is replenished from one or two energy harvesters. If the system could harvest energy continuously throughout the day then the operational lifetime could be decades. However, even with dual environmental energy sources there may be hours when the system must rely on the battery due to power consumption requirements or lack of external excitation of the energy harvesting devices. This provides two insights as they relate to the model: (1) for best performance the energy sources may need to include a combination of two energy harvesters to provide greater operational coverage and after examining the operational conditions of energy harvesters, (2) energy consumption must be calculated on an hourly basis.

Energy Source	Low (mA)	Hours of Operation	Cost	Comment
Wind Turbine	2	6pm-7am	$60	Based on Lowest Average Daily Wind Speed [38] extrapolated to hourly based on calculation from Guo [64]
Piezo Electric	0.24	6am-10am, 3pm-7pm	$100	Excitation from Morning + Evening Rush Hour[3]
Piezo Electric & Wind	0.24 – 2	19 hours	$160	
Photovoltaic Cell	3	8am-4pm	$8	Average Hours of Sunlight in Winter
PV Cell & Wind	2-3	21 hours	$68	
RF Scavenger	0.2	6am-10am, 3pm-7pm	$32	RF Signals from Morning + Evening Rush Hour[4]
RF & Wind	0.2 – 2	19 hours	$92	

Table 12: Worst Case Current Generation of Energy Sources used as part of the model

In order to determine if the energy storage device has sufficient power for the system, the active circuit time must be calculated along with the current consumption during that period. The active circuit time and current consumption are component dependent. In the case of the MCU, it generally operates in parallel with the other components, effectively doubling the active time duration. These values combined with the capacity of the energy storage device allows one to determine if there is sufficient time to recharge the super-capacitor between updates. Assuming constant current discharge, the time to recharge the capacitor is

$$t = C * \frac{\Delta v}{I}$$

Where t is the charge or discharge time, C is the capacitance of the super-capacitor, Δv is the voltage drop after operation of the circuit, and I is the current consumed during the active duration. If there is not enough time then the use of the energy harvesting based power source is reduced to every second or every third update with the battery relied upon for the other

[3] This assumes the bridge must be moderately loaded to sufficiently excite the piezo harvester

[4] The actual scavenger device works at 915MHz which is not as common as 2.4GHz (Wi-Fi). It is assumed that sufficient RF energy is available as the concepts are tested on ability to run off of the low power of the energy source.

updates. This in turn allows one to calculate the amount of current consumed on an hourly basis which is one of the values required to calculate the operational lifetime of the battery.

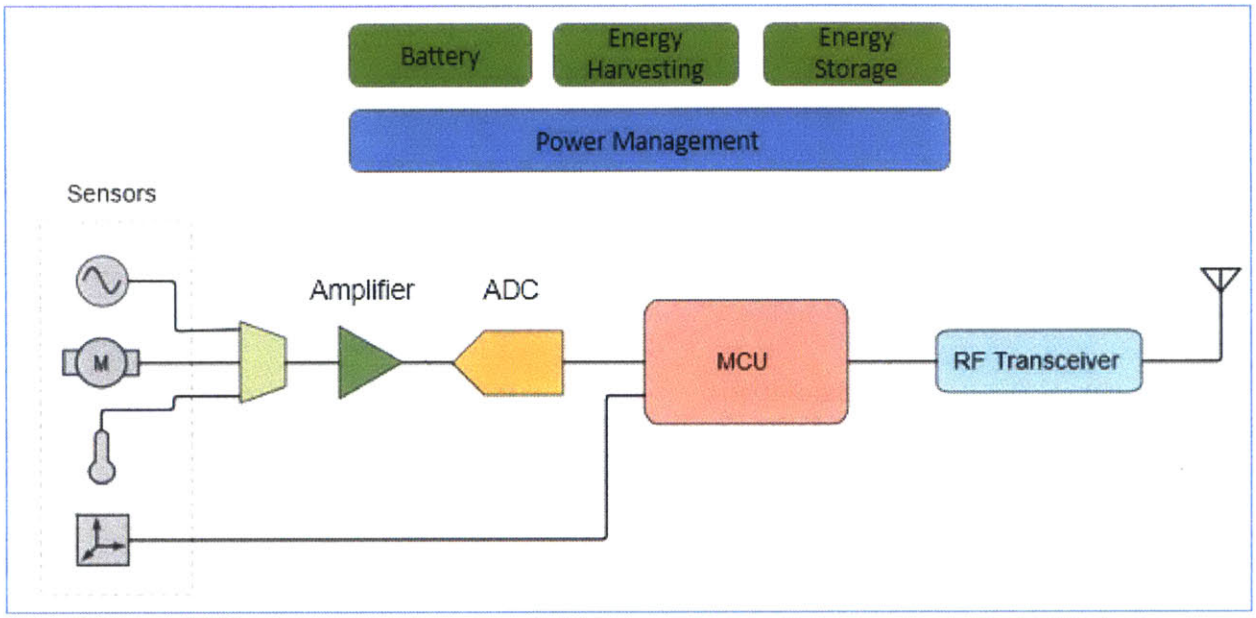

Figure 31: A generic wireless sensor node with power management and energy sources

Another aspect of calculating active circuit time and current consumption is data transmission rate for the RF Transceiver. This component is only active when it is receiving or transmitting data. In order to transmit a dataset it must first prepare a connection with the gateway, transmit the data and close the connection. This requires both transmission and reception of data. The primary driver of how quickly the transmission occurs is the data rate; the faster the data rate, the sooner the device can go to sleep. Thus in order to calculate the active time for the RF Transceiver, one must calculate the number of bytes of data to be sent for that update. The number of bytes sent is dependent on the data generated by the sensors and on the algorithms (if any are used).

To understand the impact of the RF network design on operational lifetime, the Zakim Bridge [65] in Boston, MA was selected for consideration. It is a cable-stayed bridge with a length of 436m, a width of 56m, a height of 82m, and a 12m clearance below deck. By utilizing a two-tier hierarchical network, the gateway nodes can be placed at intervals on the length of the deck sides where large PV Cells and rechargeable batteries will enable 24 hour operation. Given the width of the deck, 28m from the edge to the center point, both network protocols (detailed in Table 10) have the range to cover the distance and the capacity to handle tens to hundreds of nodes per gateway. This allows the model to be simplified by excluding the gateway portion, focusing only on the wireless sensor nodes and transmission to and from the gateway node.

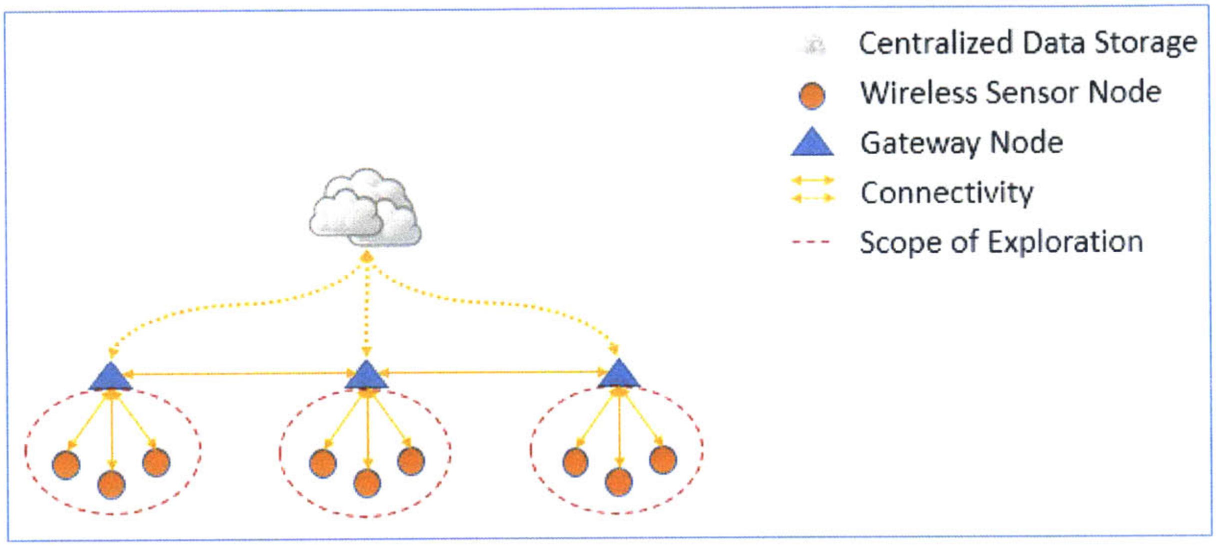

Figure 32: Two Tier Hierarchical Network

Even with multiple sensor readings and an update every 1 minute lasting 5 seconds, the system will spend 92% of the time asleep. During this time the integrated circuit components will consume standby current. In the model, this current will be drawn from the battery. Now, with knowledge of the standby current, the active current, and the active duration, it is possible to calculate the expected lifetime of the battery.

Components and their Parameters

	ZigBee/ADF7242	DASH7/ADF7023	Units
Transmit Current (0dBm)	19.6	12.2	mA
Receive Current	19	12.8	mA
Standby Current	0.3	0.3	µA
Data Rate	250	28	kbps
Cost	2.70	4	$

Table 13: RF Transceiver Part Performance

	ADXL362	Units
Active Current	4.5	µA
Standby Current	0.27	µA

Number of Bytes	12	B
Duration of Reading	0.1	s
Cost	4.89	$

Table 14: Vibration Part Parameters

	ATSAM3N4A	ADuCM350	Units
Active Current	180	400	µA/MHz
Frequency	24	16	MHz
Active Current @ Frequency	4.3	6.4	mA
Standby Current	1.5	1.6	µA
Cost	2.96	15.73	$

Table 15: Processor Part Parameters

	AD7980/ADA4805	ADuCM350 (Internal)[5]	Units
ADC Active Current	2	2	mA
ADC Standby Current	0.35	0	µA
Amp Active Current	470	470	µA
Amp Standby Current	1.3	0	µA
Number of Bytes	4	4	B
Duration of Reading	0.1	0.1	s
Cost	22.15	0	$

Table 16: ADC/Amplifier Signal Conditioning Part Parameters (for Displacement and Strain measurements)

	AD5933	ADuCM350 (Internal)	Units
Active Current	10	8.8	mA
Standby Current	0.7	0	µA
Number of Bytes	1024	1024	B
Duration of Reading	3	3	s
Cost	30.76	0	$

Table 17: Impedance Part Parameters (for Crack Detection or Corrosion Measurements)

	SHT21	Units
Active Current	300	µA
Standby Current	0.15	µA
Number of Bytes	4	B
Duration of Reading	0.1	s
Cost	5.84	$

Table 18: Temperature & Humidity Part Parameters

[5] It was not possible to discern the active current values from the ADuCM350 datasheet so the AD7980 and ADA4805 values were used.

Other Variables

Two more variables must be discussed. The first is the type of network protocol used. As noted in Table 10, there are two "RF Concepts" that were selected. DASH7 has lower power and longer range but slower data rate while ZigBee operates at a higher frequency and has shorter range but is available globally for use in the 2.4GHz band. The size of the packets for each protocol affect the number of frames that must be sent to transmit the payload when combined with the data rate determines the length of time the RF Transceiver is operating when transmitting the payload.

The second variable is the use of algorithms. For the purpose of this model, an algorithm is used to compress data to a much smaller dataset. For example, the root mean square value of a dataset may be calculated and transmitted instead of transmitting the larger dataset. In the model, if the use of algorithm is set, the number of bytes is reduced by 80% and the length of time the processor is active increases by 33%. These are arbitrary values used to determine if there is an impact from using algorithms.

The Two Concepts

With the individual components of the wireless sensor node identified, it is possible to populate the concepts with off the shelf components detailed above. In Concept 2, the ADuCM350 incorporates the signal conditioning functionality of the Amplifier, Analog to Digital Converter, and Impedance to Digital Converter. It also contains a small, dedicated Digital Signal Processor (DSP) for quickly converting the data from the internal Impedance to Digital Converter into the Real and Imaginary values of the measured impedance. This signal conditioning functionality is within the Autonomous Analog Front End (AFE) which allows it to gather data while the processor is in a low power mode.

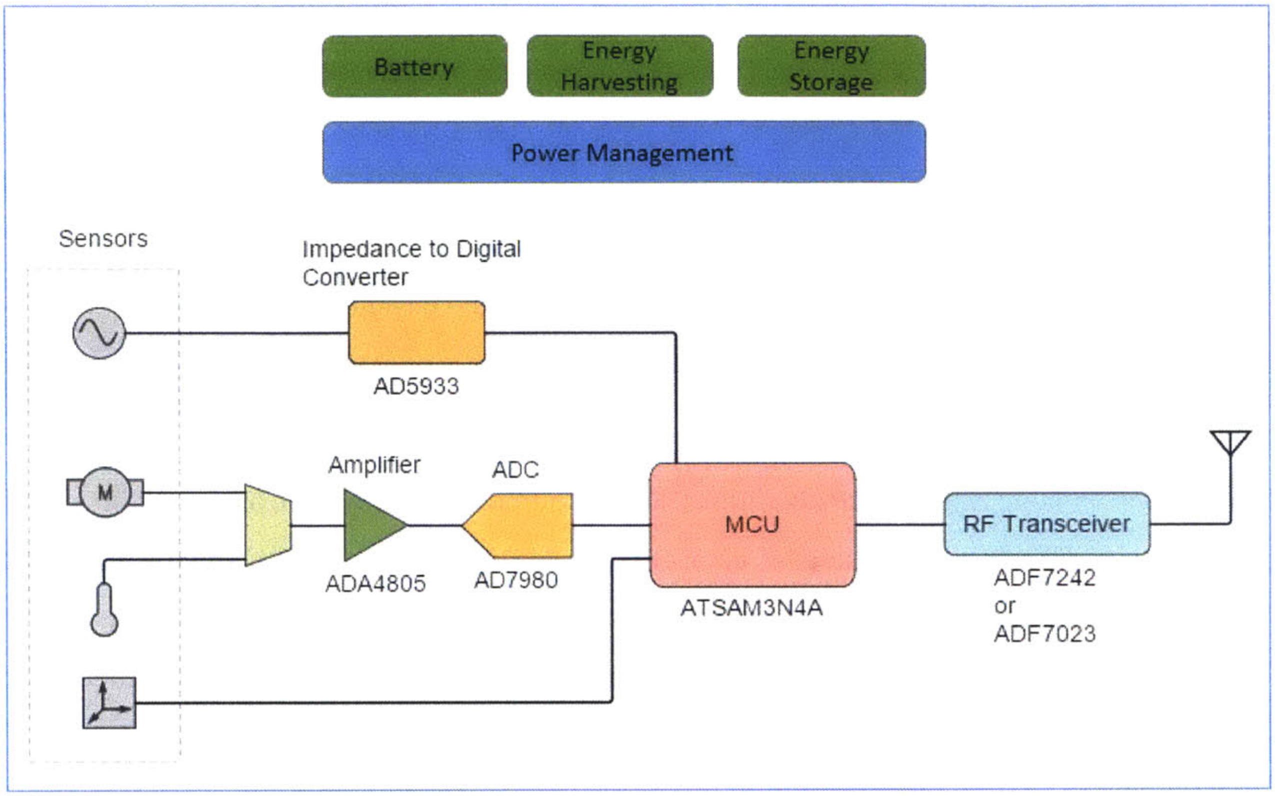

Figure 33: Concept 1 - Discrete Signal Conditioning Wireless Sensor Node with Components

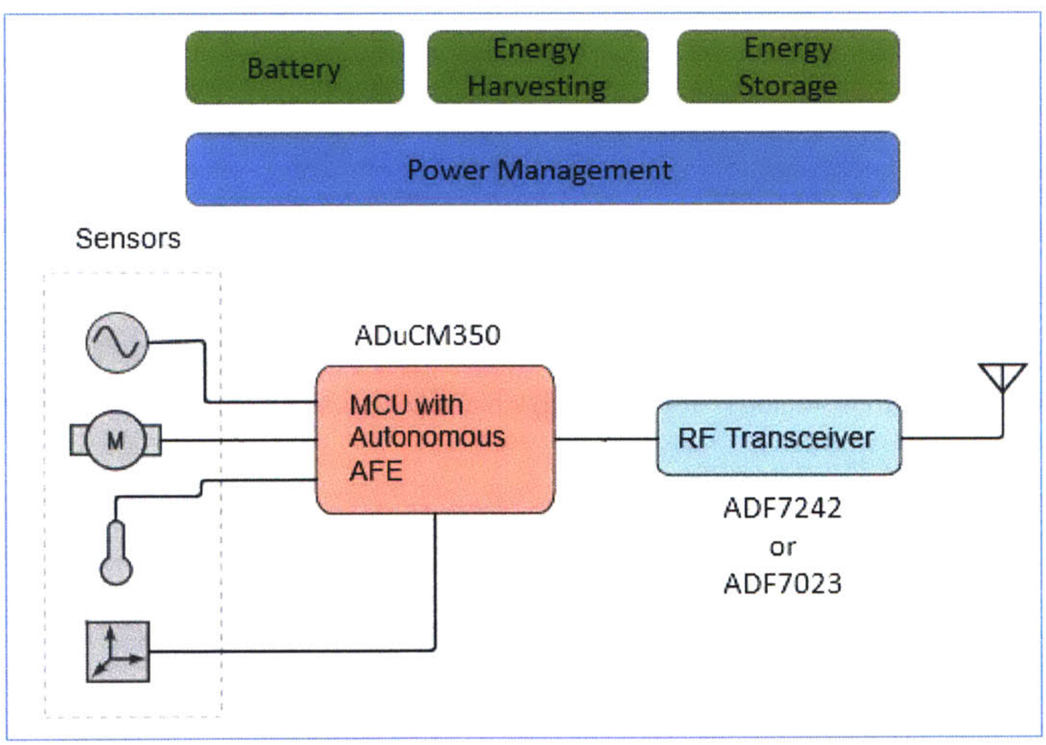

Figure 34: Concept 2 - Integrated Signal Conditioning Wireless Sensor Node with Components

The Cost Model

The final modelling piece is to determine the cost model. For both concepts, it was calculated by using the 1-unit price of each component found on various product distributor websites including Mouser, Digi-Key, Octopart, or Newark. It is assumed that data acquisition components (e.g. ADC and Amplifier, Impedance to Digital Converter) can handle 2 sensor sources by multiplexing the signals. This means only 1 component is required for every 2 phenomena measured of a particular type.

Step 6 – Generate the Tradespace

With the design vector linked to the attributes and the cost of each concept determined, it is now possible to generate the tradespace. A program to iterate through all the permutations was written in C# using Visual Studio 2013. It contained models for each component and energy source.

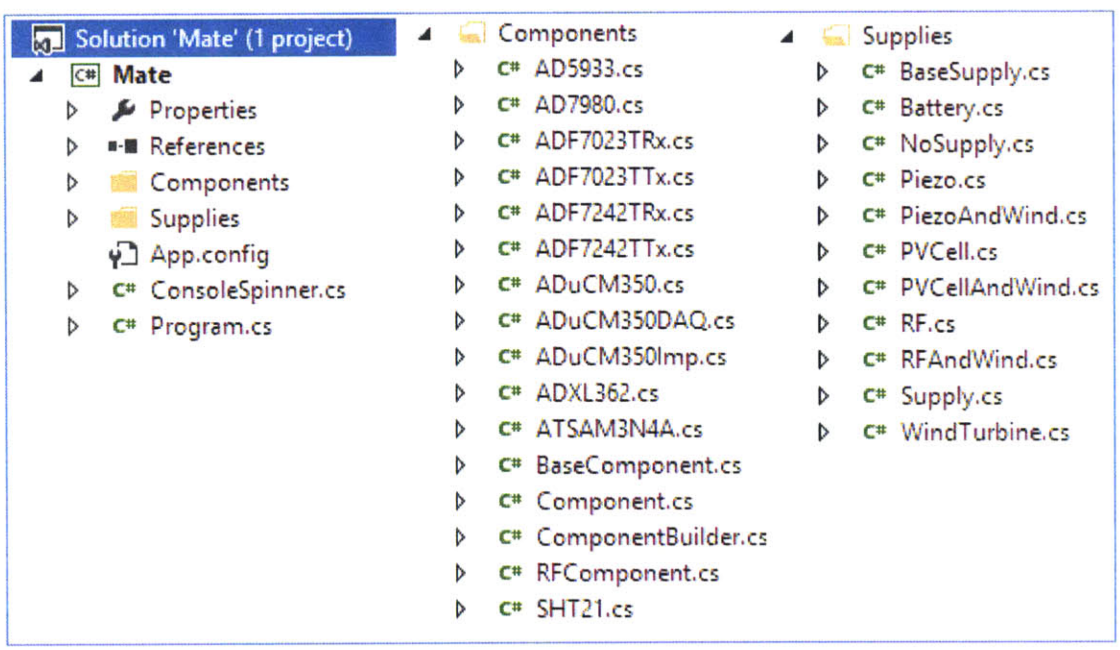

Figure 35: List of Classes in C# program for generating the tradespace

The first tradespace that was run generated more than 1,000,000 rows of data and each row had 20+ cells. It took about 12 minutes to run. After examining the results, the number of phenomena were reduced from 27 to 9. This dramatically reduced the run time to less than 30 seconds, producing nearly 45,000 rows of data.

Step 7 – Exploring the Tradespace

After generating the tradespace data, it was imported into MATLAB and processed to extract the charts below. These charts reflect the key attributes, concepts and design variables.

Concept 1 versus Concept 2

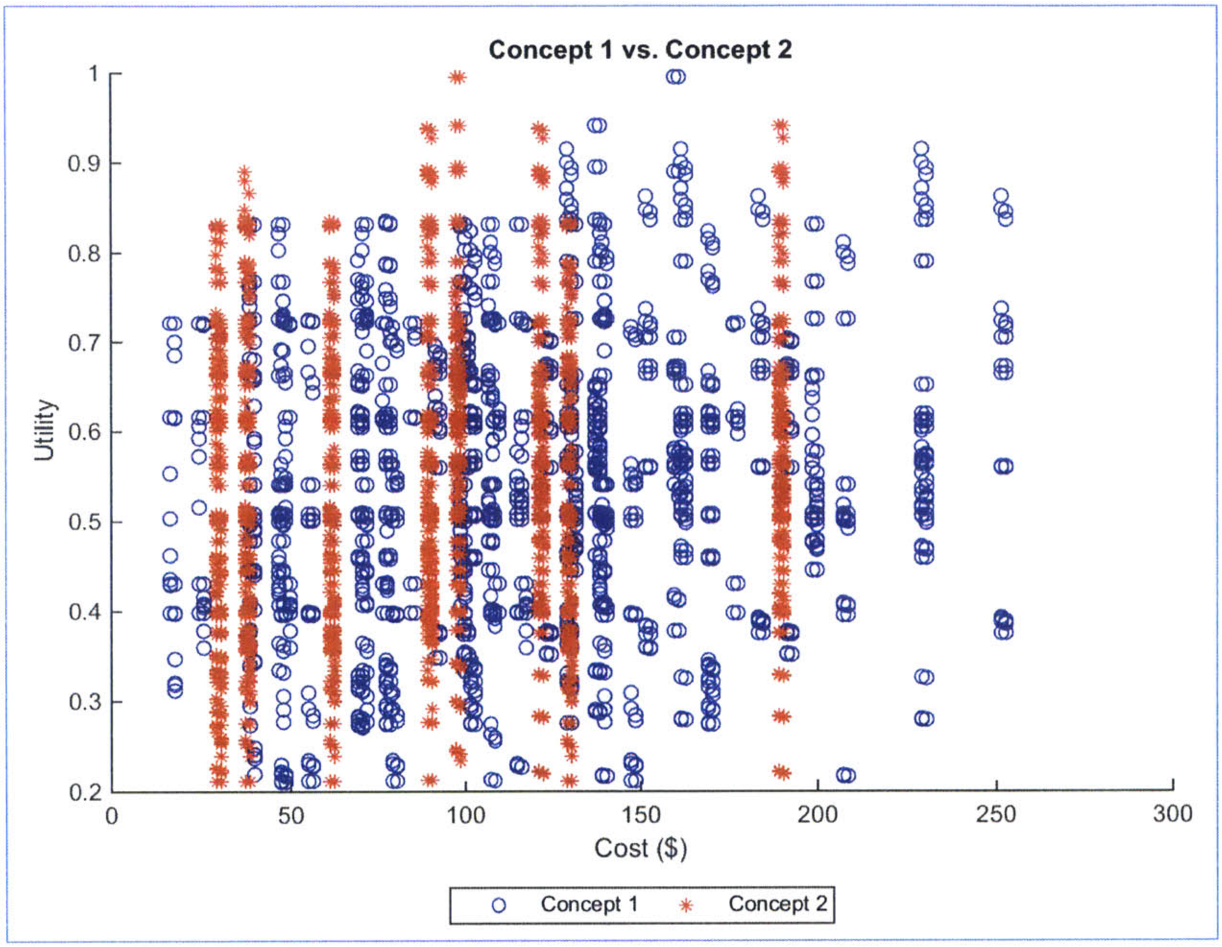

Figure 36: Performance of Concept 1 versus Concept 2

From Figure 36 it is clear that Concept 2, the integrated solution, met all the attribute requirements by scoring a 1.0 on utility and had the lowest cost by about $60. This is not much of a surprise because the integrated solution contains two parts (the Impedance to Digital Converter and the Analog to Digital Converter) which together cost $52 while the integrated solution itself is $15.

Algorithms

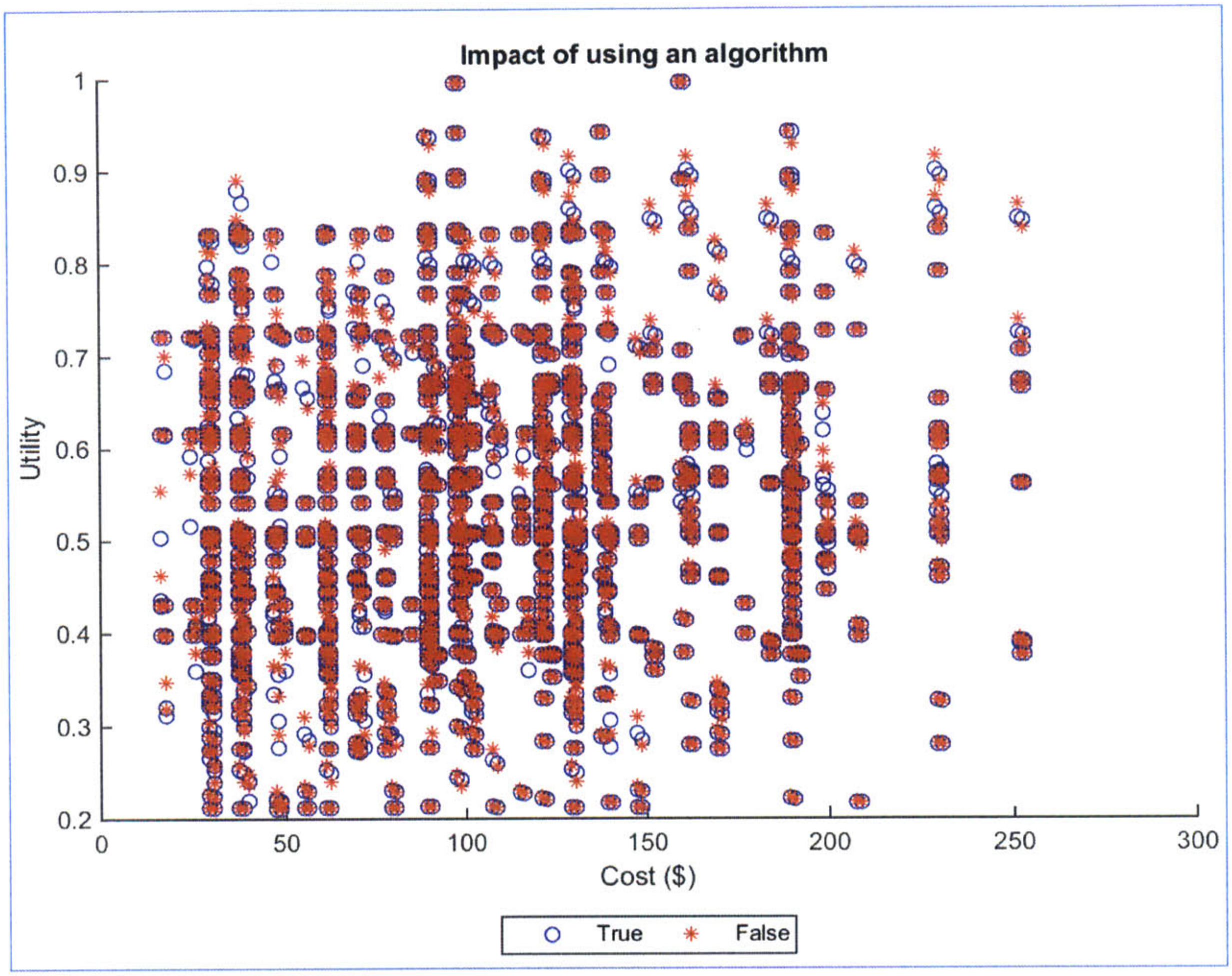

Figure 37: Impact of using an algorithm

Based on the results in Figure 37 there is little difference between running with algorithms and without. Given the low volume of data and the high frequency of transmissions, it's most likely the biggest overhead is initiating the transmission rather sending the data. This means sending 1 byte or 80 bytes of payload costs nearly the same so why not send 80 bytes? There are several examples in Figure 37 where the values do not line up with not using an algorithm having greater utility. This may be attributed to lower overhead as an algorithm is not extending the active duration of the microprocessor. In other words with small datasets, running an algorithm to extract value may be more expensive than not running it.

Wireless Protocols

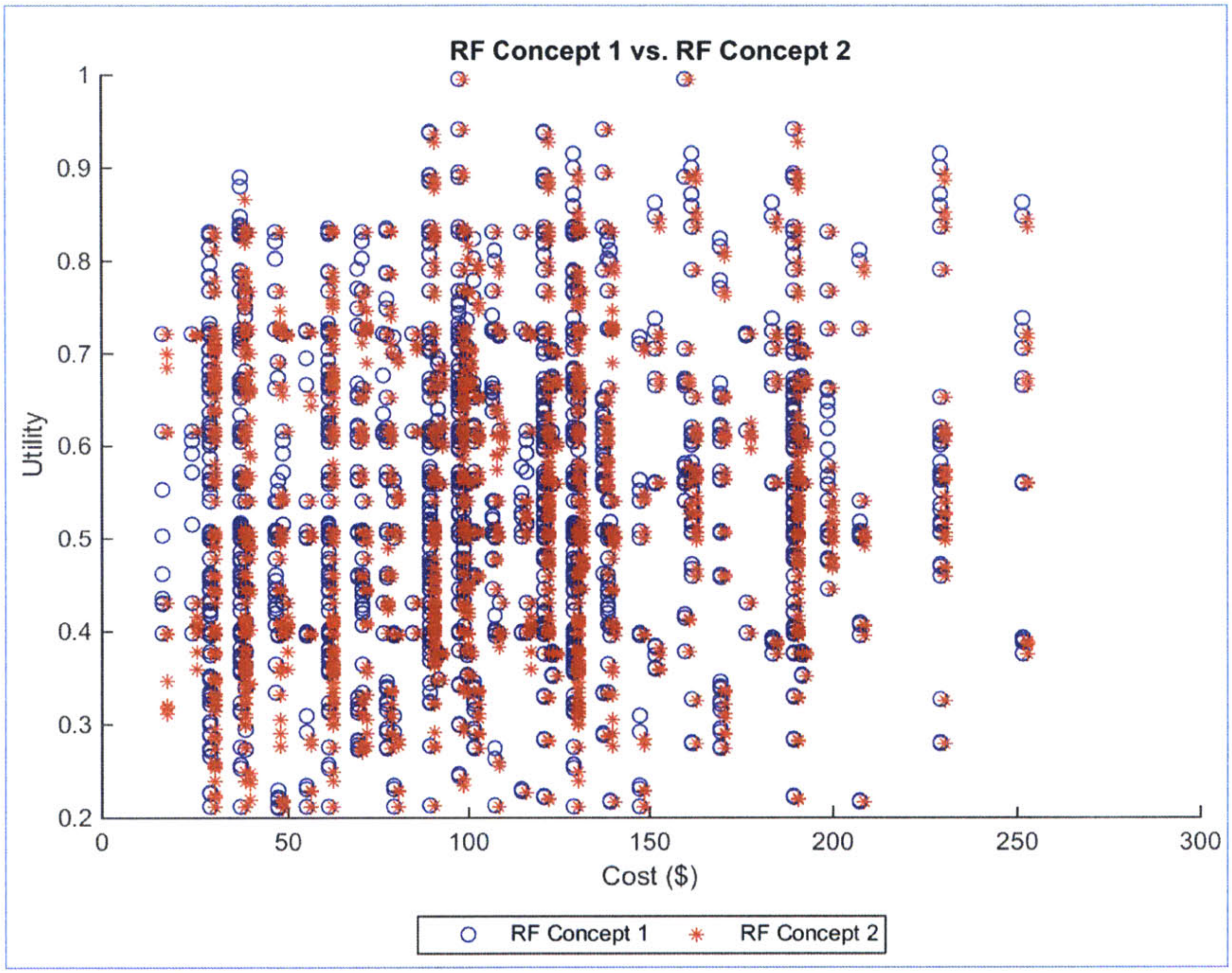

Figure 38: Performance of RF Concept 1 versus RF Concept 2

Figure 38 shows little difference between the two different RF Protocols that are available. The slight horizontal shift is due to the price difference between the two RF Concepts.

Operational Lifetime

Battery Operation

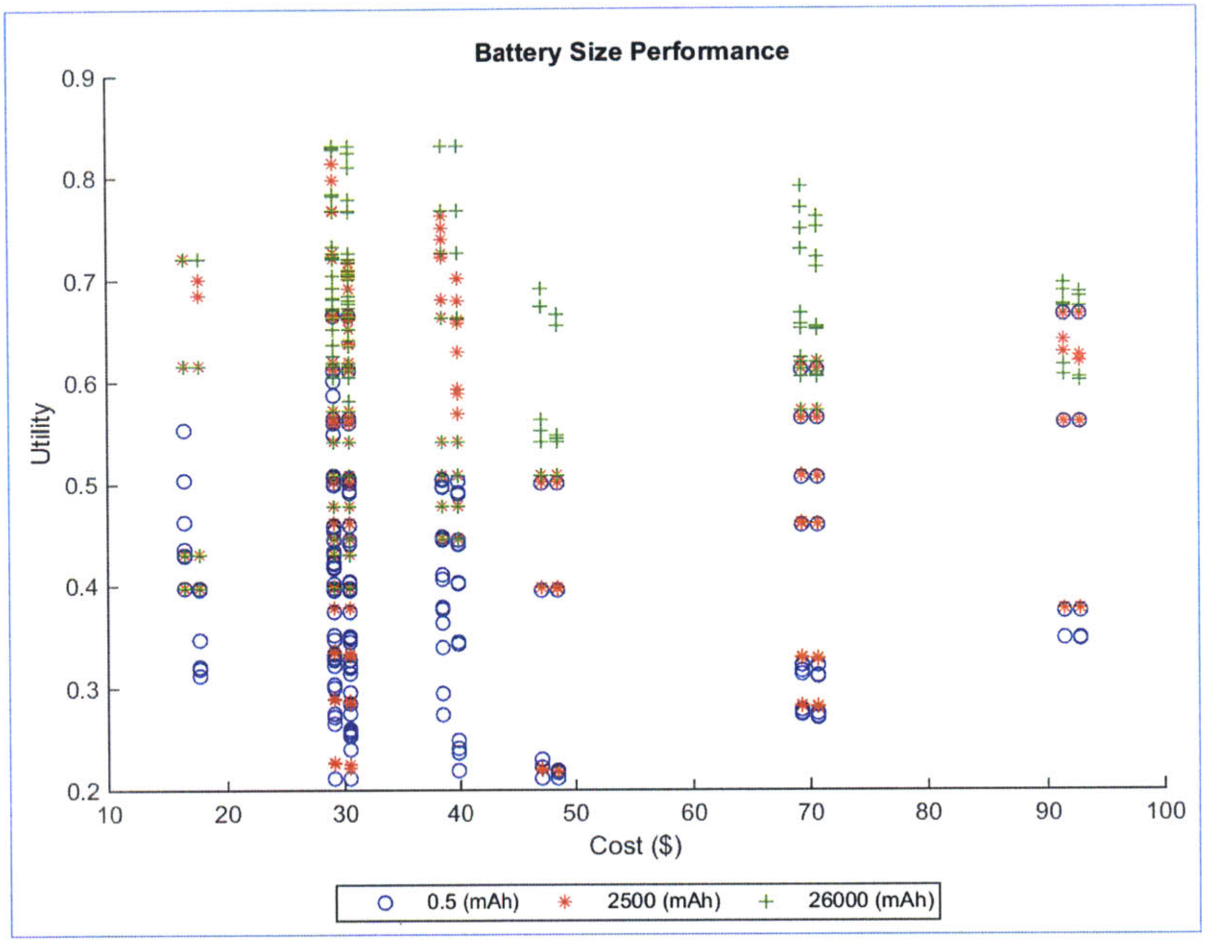

Figure 39: Battery Size Performance

The best utility achieved by battery alone is ~0.825. There is an iron triangle in play here between Operational Lifetime, Number of Updates per Hour, and Number of Phenomena Measured. As the number of phenomena measured increases, the operational lifetime decreases unless the number of updates is reduced. This in turn reduces the overall utility value. It's clear that even with 26000mAh capacity, the largest battery will not last for 10 years on its own. One option is to add energy harvesting to complement the battery. Another would be to reduce the update rate from once every minute to once every 5 minutes. This would lead to a 10 year operational lifetime on the largest battery. Another option would be to optimize the update process by determining the most appropriate update rate on a per phenomenon basis. In this way the frequency of the most expensive measurement may be reduced to extend the battery life. An experiment to validate this was conducted with the existing model by reducing the active duration to 0.05s from 3s. This is equivalent to conducting the measurement every hour instead of every minute. With that, the largest battery can now reach 10 years of operational lifetime with the maximum phenomena measured, with all but impedance measured every minute and with impedance measured every hour. This seems a reasonable optimization as corrosion or crack detection won't change significantly within an hour.

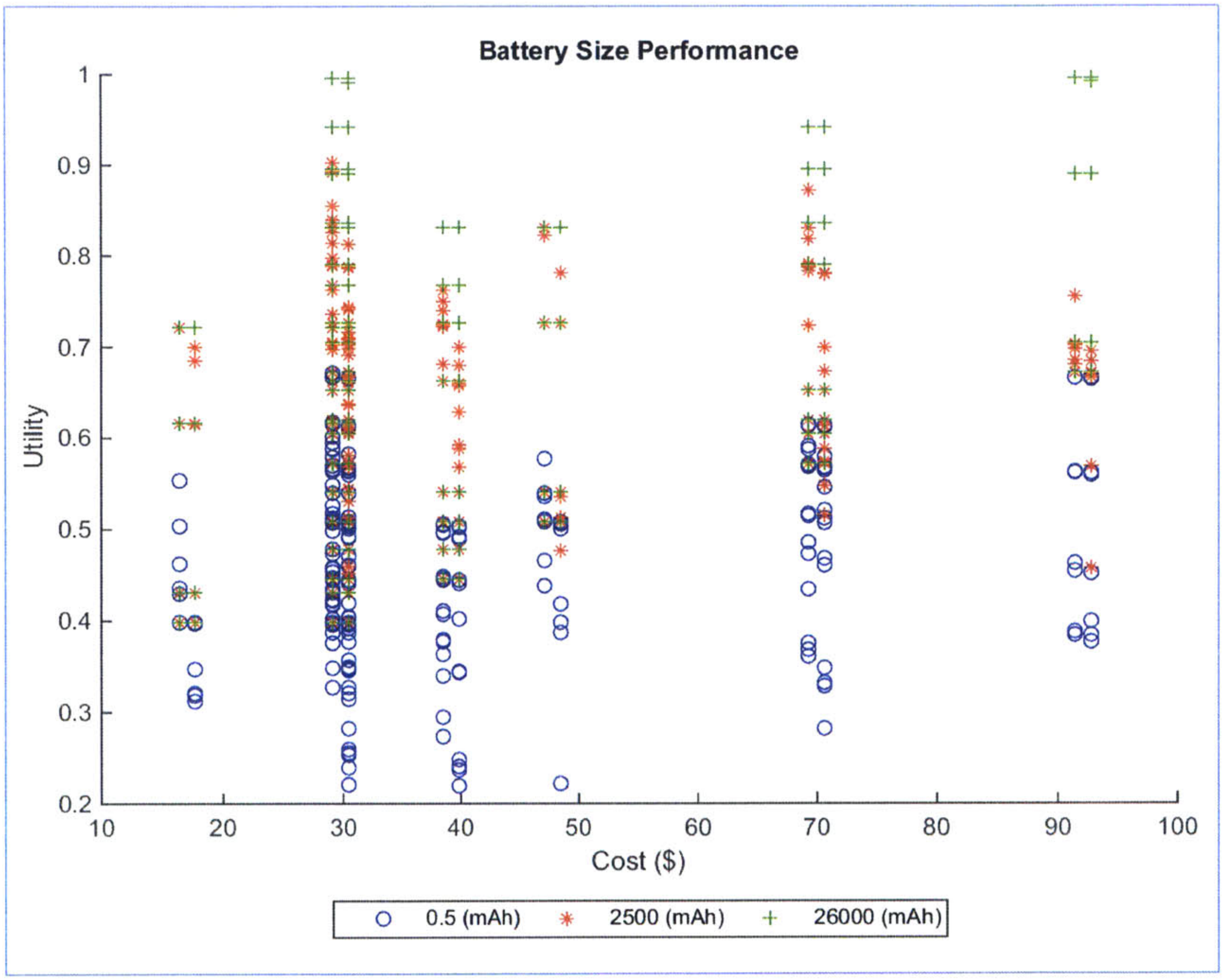

Figure 40: Battery performance with impedance measurement every hour

Energy Harvesting Concepts

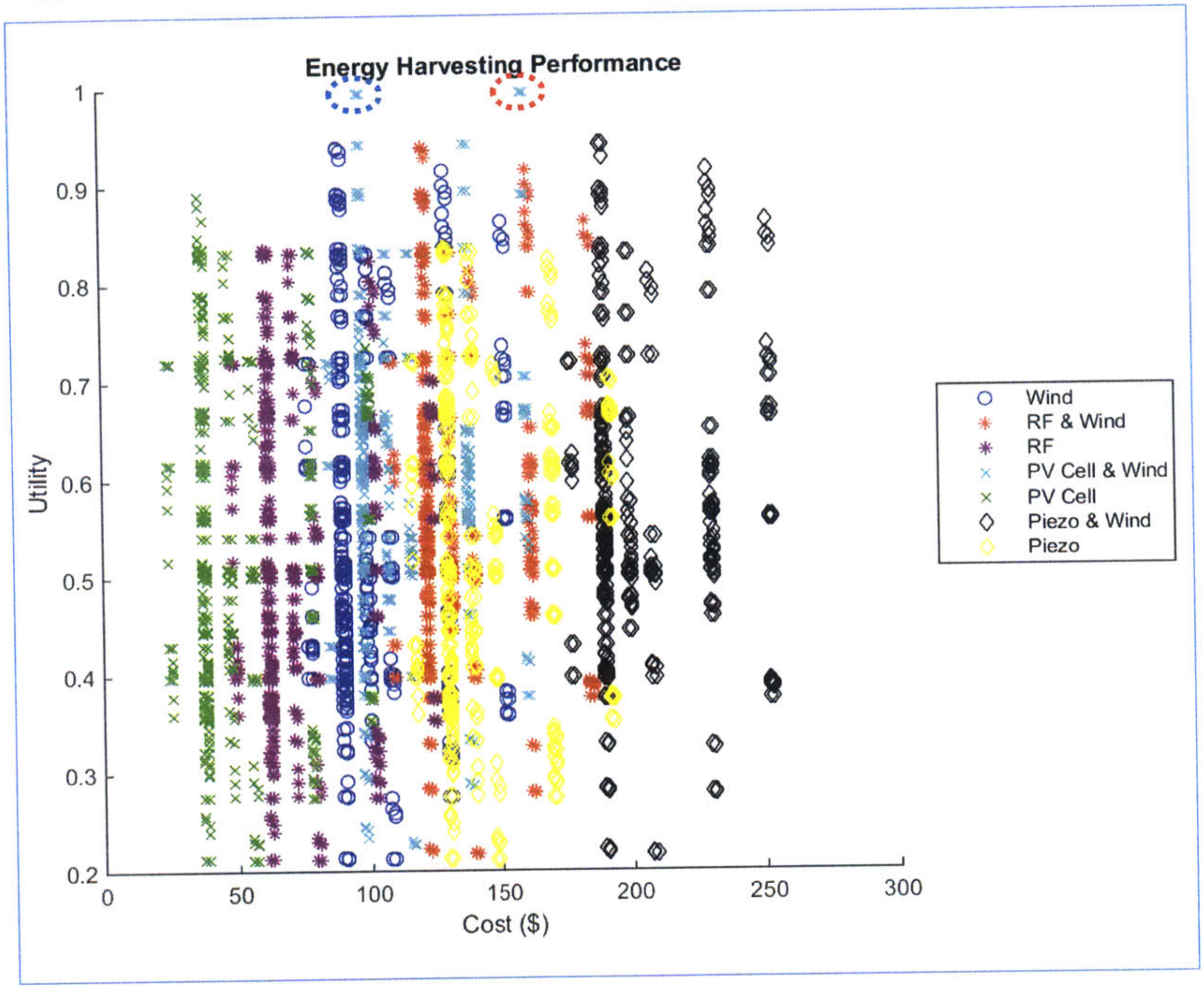

Figure 41: Energy Harvesting Impact on Performance of Concepts

Each concept achieves a utility value of 1.0 when combined with PV Cell & Wind Turbine energy harvesting and a large lantern (26000mAh) battery. This reinforces the need to provide at least 3 energy sources, 2 renewable and 1 electrochemical, to ensure longevity of the wireless node. However, if the longest running measurement with the largest power requirements is run less frequently, it may be possible to utilize only 1 electrochemical source and 1 renewable source. This can be seen in Figure 42 where the large lantern battery (26000mAh capacity) combined with a PV Cell will contribute to a utility value of 1.0 when the impedance measurement is just once an hour.

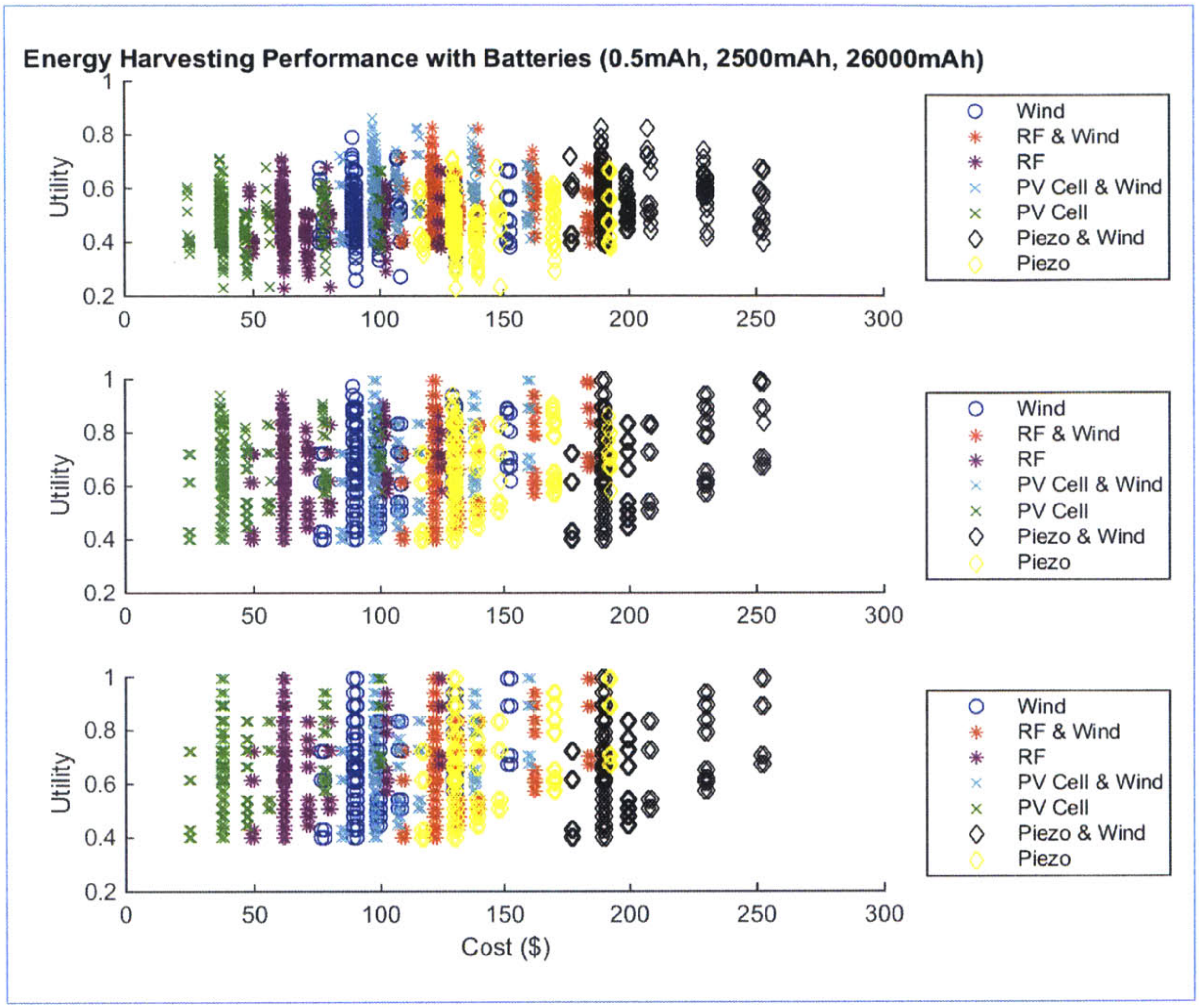

Figure 42: Energy Harvesting Impact on Concept Performance Broken Out by Battery Size with Hourly Impedance Measurement

Conclusions

Concept 2 provided equivalent performance but superior cost by integrating various components into one product. Surprisingly, use of an algorithm does not improve performance. This may be due to the small size of the data gathered and transmitted. The selected RF protocols had no effect on either concept. However, a valuable lesson was learned while preparing the model. There is a common misperception that a faster data rate is more expensive however the sooner the transceiver completes a transmission, the sooner it can go back to sleep thus the faster transceiver uses less power overall. Another misconception is that the RF Transceiver is the most power hungry device in a wireless sensor node; however as evidenced by the improvement in overall operational lifetime when impedance is measured less frequently, even if a device uses 50% less power, it will have a greater effect on performance if it is active for 10x the duration than the RF transceiver.

From the performance of the batteries with energy harvesting, it is clear that large capacity batteries are preferred if the form factor permits their volume. It would have been difficult for either concept to achieve 10 years or more in operational lifetime without such a large battery. It was also very clear that the optimization of the update rate on a per phenomenon basis is necessary to extend the operational lifetime of the wireless sensor node. Similarly, in order to reduce the number of renewable energy sources required, optimization of the update rate is necessary. Significantly, this change in the impedance measurement rate also decreases the cost of the node from $100 to $40.

Future Work

In this analysis the first step, stakeholder identification, of Multi-Attribute Tradespace Exploration was skipped which in turn meant no interviews were conducted. This weakens the conclusions of the research as the values identified were based on subjective interpretation of SHM requirements in literature. As noted by Ross & Rhodes in their short course on MATE [43], such short-cuts can lead to incorrect results. Any future work must be grounded in stakeholder value identification using the techniques recommended by MATE.

As the research work concluded several enhancements to the model become clear:

1. Custom frequency of operation for each sensor
    a. Not all sensors need to run every minute every hour c.f. the impedance sensor versus the vibration sensor. Capturing more realistic scenarios would further enhance the value of the research results
2. Improve the RF network model to remove the 2-layer limitation thus allowing it to model the effects of mesh routing and always on nodes
3. Improve the RF network model to take into account for signal loss through the bridge structure
    a. Near line of sight was assumed with a 50% degradation in range as it simplifies the model, however this is an optimistic assumption. A better model would incorporate estimates for signal degradation through concrete/steel structures which would in turn lead to a more complicated RF network design
4. Improve the model for battery leakage over its lifetime
    a. It was assumed that a battery would lose 10% of its energy over its lifetime
5. Investigate in greater depth the impact of large data volumes on performance especially if algorithms are applied.
    a. The model already produced low volume data so the effect of algorithms were negligible.
6. Improve the power management model by ensuring the standby current is drawn from the storage device and then the battery
    a. The model currently has the standby current deplete the battery even if the storage device has capacity

Finally, working with the stakeholders identified as part of Step 1 of the MATE process, identify a bridge to monitor. This will require the design and fabrication of several dozen wireless sensor nodes to verify the findings of this research.

References

[1] J. Brownjohn, "Structural health monitoring of civil infrastructure," *Philosophical Transactions of The Royal Society A,* vol. 365, no. 12, pp. 589-622, 2007.

[2] C. Farrar and W. Keith, "An introduction to structural health monitoring," *Philosophical Transactions of the Royal Society of London A: Mathematical, Physical and Engineering Sciences,* vol. 365, no. 1851, pp. 303-315, 2006.

[3] NDT, "A Brief History of AE Testing," [Online]. Available: https://www.nde-ed.org/EducationResources/CommunityCollege/Other%20Methods/AE/AE_History.htm. [Accessed 26 04 2015].

[4] D. S. Carder, "Observed Vibrations of Bridges," *Bulletin of the Seismological Society of America,* vol. 27, no. 4, pp. 267-303, 1937.

[5] C. S. Ling, D. Hewitt, S. G. Burrow, L. Clare, D. A. W. Barton, D. M. Wells and N. A. J. Lieven, "Technological challenges of developing wireless health and usage monitoring systems," in *Health Monitoring of Structural and Biological Systems*, San Diego, 2013.

[6] J. Lynch, "An overview of wireless structural health monitoring for civil structures," *Philosophical Transactions of The Royal Society,* pp. 345-372, 2007.

[7] J. Park, H. Jung, H. Jo and B. Spencer, "Feasibility Study of Micro-Wind Turbines for Powering Wireless Sensors on a Cable-Stayed Bridge," *Energies,* vol. 5, pp. 3450-3464, 2012.

[8] K. Worden and J. Dulieu-Barton, "An overview of intelligent fault detection in systems and structures," *STRUCTURAL HEALTH MONITORING,* vol. 3, no. 1, pp. 85-98, 2004.

[9] Federal Highway Administration, "2010 Status of the Nation's Highways, Bridges, and Transit: Conditions and Performance," 2010. [Online]. Available: http://www.fhwa.dot.gov/policy/2010cpr/execsum.htm#c3h. [Accessed 26 04 2015].

[10] ASCE, "2013 Report Card for Americas' Infrastructre," 2013. [Online]. Available: http://www.infrastructurereportcard.org/a/documents/Bridges.pdf. [Accessed 26 04 2015].

[11] K. Wardhana and F. Hadipriono, "Analysis of Recent Bridge Failures in the United States," *Journal of Performance of Constructed Facilities,* vol. 17, no. 3, pp. 144-150, 2003.

[12] G. T. Webb, P. J. Vardanega, P. R. A. Fidler and C. R. Middleton, "Analysis of Structural Health Monitoring Data from Hammersmith Flyover," *Journal of Bridge Engineering,* vol. 19, no. 6, p. 05014003, 2014.

[13] D. Inaudi, "Overview of 40 Bridge Structural Health Monitoring Projects," [Online]. Available: www.smartec.ch/content/download/678/5017/file/c197.pdf. [Accessed 26 04 2015].

[14] M. Modares and N. Waksmanski, "Overview of Structural Health Monitoring for Steel Bridges," *Practice Periodical on Structural Design & Construction,* vol. 18, no. 3, pp. 187-191, 2013.

[15] S. PARK, C. YUN and D. INMAN, "Structural health monitoring using electro-mechanical impedance sensors," *Fatigue & Fracture of Engineering Materials & Structures,* vol. 31, no. 8, pp. 714-724, 2008.

[16] G. Park and D. Inman, "Structural health monitoring using piezoelectric impedance measurements," *Philosophical Transactions of the Royal Society of London A: Mathematical, Physical and Engineering Sciences,* vol. 365, no. 1851, pp. 373-382, 2007.

[17] G. Park, H. H. Cudney and D. Inman, "Impedance-Based Health Monitoring of Civil Structural Components," *Journal of Infrastructure Systems,* vol. 6, no. 4, pp. 153-160, 2000.

[18] Analog Devices, "AD5933, a 12 Bit Impedance Converter Network Analyzer," 2005. [Online]. Available: http://www.analog.com/AD5933. [Accessed 28 04 2015].

[19] S. Kim, D. Frangopol and B. Zhu, "Probabilistic Optimum Inspection/Repair Planning to Extend Lifetime of Deteriorating Structures," *Journal of Performance of Constructed Facilities,* vol. 25, no. 6, pp. 534-544, 2011.

[20] S. Park, B. L. Grisso, D. L. Inman and C. Yun, "MFC-based structural health monitoring using a miniaturized impedance measuring chip for corrosion detection," *RESEARCH IN NONDESTRUCTIVE EVALUATION,* vol. 18, no. 2, pp. 139-150, 2007.

[21] Wikipedia, "Linear variable differential transformer," [Online]. Available: http://en.wikipedia.org/wiki/Linear_variable_differential_transformer. [Accessed 28 04 2015].

[22] Measurement Specialties, "Economy Series LVDTs," [Online]. Available: http://www.meas-spec.com/downloads/E_Series.pdf. [Accessed 28 04 2015].

[23] Y. T. S. G. B. Yao, "Crack detection and characterization techniques—An overview," *Structural Control and Health Monitoring,* vol. 21, no. 12, pp. 1387-1413, 2014.

[24] R. O'Reilly, A. Khenkin and K. Harney, "Sonic Nirvana: Using MEMS Accelerometers as Acoustic Pickups in Musical Instruments," *Analog Dialogue,* vol. 43, no. 01, pp. 11-14, 02 2009.

[25] Omega, "Introduction to Fiber Optics Temperature Measurement," [Online]. Available: http://www.omega.com/prodinfo/fiberoptictemp.html. [Accessed 28 04 2015].

[26] Sensor Online, "Humidity/Moisture Choosing a Humidity Sensor: A Review of Three Technologies," 01 07 2001. [Online]. Available: http://www.sensorsmag.com/sensors/humidity-moisture/choosing-a-humidity-sensor-a-review-three-technologies-840. [Accessed 28 04 2015].

[27] Sensirion, "SHT2x Humidity and Temperature Sensors," [Online]. Available: http://www.sensirion.com/en/products/humidity-temperature/humidity-temperature-sensor-sht2x/. [Accessed 12 04 2015].

[28] H. Park, Y. Shin, S. Choi and Y. Kim, "An Integrative Structural Health Monitoring System for the Local/Global Responses of a Large-Scale Irregular Building under Construction," *Sensors (14248220)*, vol. 13, no. 7, pp. 9085-9103, 2013.

[29] Analog Devices, "ADuCM350," [Online]. Available: http://www.analog.com/ADuCM350. [Accessed 28 04 2015].

[30] ARM, "Cortex-M4 Processor," [Online]. Available: http://www.arm.com/products/processors/cortex-m/cortex-m4-processor.php. [Accessed 28 04 2015].

[31] ZigBee, "ZigBee Alliance," [Online]. Available: http://www.zigbee.org/. [Accessed 28 04 2015].

[32] DASH7 Alliance, "DASH7 Technical Overview Webinar," 02 12 2009. [Online]. Available: http://www.slideshare.net/Dash7Alliance/dash7-technical-overview-webinar. [Accessed 28 04 2015].

[33] Dash7 Alliance, "DASH7 Technical Overview Webinar," 02 12 2009. [Online]. Available: http://www.slideshare.net/Dash7Alliance/dash7-technical-overview-webinar. [Accessed 12 04 20015].

[34] Y. Tan and S. Panda, "Review of Energy Harvesting Technologies for Sustainable WSN," 14 12 2010. [Online]. Available: http://www.intechopen.com/books/sustainable-wireless-sensor-networks/review-of-energy-harvesting-technologies-for-sustainable-wsn. [Accessed 28 04 2015].

[35] W. Serdijn, A. Mansano and M. Stoopman, "Chapter 4.2 - Introduction to RF Energy Harvesting," in *Wearable Sensors*, Oxford, Academic Press, 2014, p. 2990322.

[36] Mide, "QuickPack QPK-1001," [Online]. Available: http://www.mide.com/pdfs/quickpack-qpk-1001-datasheet.pdf. [Accessed 28 04 2015].

[37] L. Mateu, T. Drager, I. Mayordomo and M. Pollak, "Chapter 4.1 - Energy Harvesting at the Human Body," in *Wearable Sensors: Fundamentals, Implementation and Applications*, Oxford, Academic Press, 2014, p. 235–298.

[38] Weather Spark, [Online]. Available: https://weatherspark.com/averages/29794/Boston-Massachusetts-United-States. [Accessed 14 04 2015].

[39] Mini Solar, "Mini Solar Educational Wind Turbine Kit," [Online]. Available: http://minisolarworld.com/products/products/educational-wind-turbine-kit-mt-150-vertical-type/. [Accessed 28 04 2015].

[40] N. P. Diller, "Utilizing multiple attribute tradespace exploration with concurrent design for creating aerospace systems requirements.," MIT, Cambridge, 2002.

[41] A. M. Ross, "Multi-attribute tradespace exploration with concurrent design as a value-centric framework for space system architecture and design.," MIT, Cambridge, 2003.

[42] R. Keeney, Value-Focused Thinking - A Path to Creative Decision-making, Cambridge: Harvard University Press, 1992.

[43] A. Ross and D. H. Rhodes, "Value-Driven Tradespace Exploration for System Design," 24 07 2010. [Online]. Available: http://seari.mit.edu/short_courses.php. [Accessed 12 04 2015].

[44] A. Yu, W. Yang and J. Dai, "Large-scale Structural health monitoring based on wireless sensor networks," *Applied Mechanics and Materials,* Vols. 644-650, pp. 1317-1323, 2014.

[45] T. J. Spaulding, "Tools for Evolutionary Acquisition: A Study of Multi-Attribute Tradespace Exploration (MATE) Applied to the Space Based Radar (SBR).," MIT, Cambridge, 2003.

[46] Y. Fujino and D. Siringoringo, "Recent studies on long-span bridges: Vibration control, seismic retrofit and monitoring in Japan," *Research and Applications in Structural Engineering, Mechanics and Computation*, pp. 9-16, 2013.

[47] T.-H. Yi, H.-N. Li and X.-D. Zhang, "Health monitoring sensor placement optimization for Canton Tower using immune monkey algorithm," *STRUCTURAL CONTROL AND HEALTH MONITORING,* vol. 22, no. 1, pp. 123-138, 2015.

[48] M. Whelan, M. Gangone and K. Janoyan, "Highway Bridge Assessment Using an Adaptive Real-Time Wireless Sensor Network," *IEEE SENSORS JOURNAL,* vol. 9, no. 11, pp. 1405-1413, 2009.

[49] S. Material, "Macro Fiber Composite - MFC," [Online]. Available: http://www.smart-material.com/MFC-product-main.html. [Accessed 12 04 2015].

[50] Analog Devices, "ADXL362 Micropower 3-Axis MEMS Accelerometer," [Online]. Available: http://www.analog.com/en/products/mems/mems-accelerometers/adxl362.html. [Accessed 12 04 2015].

[51] Omega, "Precision Strain Gauge," [Online]. Available: http://www.omega.com/Pressure/pdf/SGD_LINEAR1-AXIS.pdf. [Accessed 12 04 2015].

[52] Digi-Key, "HPP845E031R4 Temperature and Humidity Sensor," [Online]. Available: http://www.digikey.com/product-detail/en/HPP845E031R4/223-1144-2-ND/3945784. [Accessed 12 04 2015].

[53] Measurement Specialties, "Economy Series AC LVDT," [Online]. Available: http://www.meas-spec.com/downloads/E_Series.pdf. [Accessed 12 04 2015].

[54] R. Keeney and H. Raiffa, Decisions with Multiple Objectives - Preferences and Value Tradeoffs, Cambridge: Cambridge University Press, 1993.

[55] MiniSolar, "MT-150 Mini Wind Turbine Kit (Vertical Type)," [Online]. Available: http://minisolarworld.com/products/products/educational-wind-turbine-kit-mt-150-vertical-type/. [Accessed 12 04 2015].

[56] Perpetuum, "Vibration Energy Harvesters," [Online]. Available: http://perpetuum.com/resources/Vibration%20Energy%20Harvester_Data%20Sheet_21Oct13.pdf. [Accessed 12 04 2015].

[57] AltaDevices, "Solar Powered Wireless Sensors," [Online]. Available: http://www.altadevices.com/pdfs/sensors.pdf. [Accessed 12 04 2015].

[58] POWERCAST, "P1110 - 915MHz RF Powerharvester Receiver," [Online]. Available: http://www.mouser.com/ds/2/329/P1110-datasheet-694.pdf. [Accessed 12 04 2015].

[59] Micropelt, "Thermoelectric Generator," [Online]. Available: http://www.micropelt.com/downloads/datasheet_thermogenerator_package.pdf. [Accessed 13 04 2015].

[60] Horizon Fuel Cells, "HydroStick Hydrogen Fuel Cell," [Online]. Available: http://www.horizonfuelcell.com/#!minipak/c156u. [Accessed 13 04 2015].

[61] Allied Electrical, "Panasonic Battery Datasheet," [Online]. Available: http://www.alliedelec.com/Images/Products/Datasheets/BM/PANASONIC_BATTERIES/70197036.pdf. [Accessed 12 04 2015].

[62] Energizer, "E91 Datasheet," [Online]. Available: http://data.energizer.com/PDFs/E91.pdf. [Accessed 12 04 2015].

[63] Wikipedia, "Lantern Battery," [Online]. Available: http://en.wikipedia.org/wiki/Lantern_battery. [Accessed 12 04 2015].

[64] Z. Guo, "A simple method to downscale daily wind statistics to hourly wind data," 13 05 2013. [Online]. Available: http://arxiv.org/abs/1305.3367. [Accessed 14 04 2015].

[65] Wikipedia, "Leonard P. Zakim Bunker Hill Memorial Bridge," [Online]. Available: http://en.wikipedia.org/wiki/Leonard_P._Zakim_Bunker_Hill_Memorial_Bridge. [Accessed 18 04 2015].